Journal of Medicinal Chemistry

pubs.acs.org/jmc

Open Access

This article is licensed under CC-BY 4.0

Article

Novel Inhibitors of *Plasmodium* Phosphatidylinositol 4-kinase III*β* with Low Propensity for Resistance: Life Cycle Stage Activity and *In Vivo* Efficacy in a Humanized Mouse Malaria Infection Model

Godwin A. Dziwornu,[⋈] Mmakwena M. Mmonwa,[⋈] Dina Coertzen, Liezl Krugmann, Nicolaas Salomane, Meta Leshabane, Jean Thomas, Shante da Rocha, Janette Reader, Keabetswe Masike, Mathew Njoroge, Nicole Sevilleno, Rachael Coyle, Nonlawat Boonyalai, Emily Mayville, Marcus C. S. Lee, David A. Fidock, Lauren B. Coulson, John G. Woodland, Kathryn J. Wicht, Sandeep R. Ghorpade, Lyn-Marié Birkholtz, and Kelly Chibale*

Cite This: *J. Med. Chem.* 2025, 68, 17736−17751

Read Online

ACCESS | Metrics & More | Article Recommendations | Supporting Information

ABSTRACT: Anticancer ATP-competitive inhibitors are a promising source of new starting points for antimalarial drug discovery. Herein, we present a novel antimalarial chemotype based on the anticancer human ataxia-telangiectasia-mutated (ATM) kinase inhibitor AZD0156. This class inhibits phosphatidylinositol 4-kinase III*β* (PI4K) in the human malaria parasite *Plasmodium*, demonstrating remarkable activities against all stages of the *Plasmodium falciparum* life cycle. The current series exhibited a lower propensity for resistance and toxicity compared to previous *Plasmodium* PI4K inhibitors. The lead compound **18** was efficacious in a humanized NOD-*scid IL-2Rγnull* mouse model of *P. falciparum* malaria, with an ED_{90} value of 4.6 mg kg^{-1}.

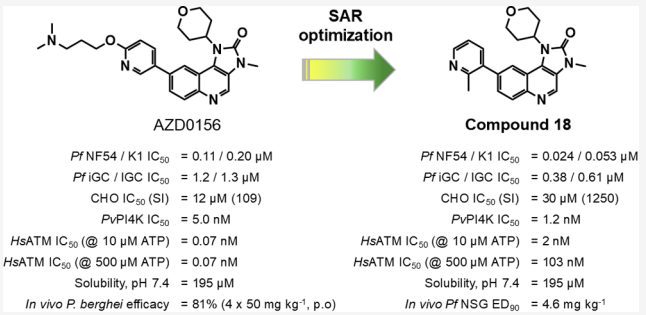

INTRODUCTION

The emergence of resistance to current antimalarial drugs hampers progress toward the control and elimination of malaria.[1,2] The artemisinin-based combination therapy (ACT) regimen is recommended as a first-line treatment for malaria.[1−3] However, resistance toward the artemisinin component compromises the future efficacy of this regimen.[4−6] The RTS,S/AS01 and R21/Matrix-M malaria vaccines, showing moderate efficacy, are expected to contribute to the control and eradication of malaria.[7,8] Seasonal malaria chemoprevention (SMC) community-based intervention is highly effective in preventing malaria in areas with seasonal transmission. In clinical trials, the SMC regimen of sulfadoxine-pyrimethamine and amodiaquine (SPAQ) was highly effective, providing up to 88% protection against infection in the first 28 days and a 61% reduction in clinical malaria 29−42 days after administration.[9] The current malaria prevention strategy focuses on long-acting oral and injectable drugs.[10]

Drug repurposing and repositioning approaches have shown potential in identifying antimalarial agents from known antiparasitic agents.[11] Similarly, several anticancer agents have shown potential to be repurposed and/or repositioned for malaria.[11,12] In spite of the safety concerns around anticancer chemotherapy, where high doses are typically administered for a prolonged period, anticancer agents have the potential to be repurposed and/or repositioned against acute malaria, whose treatment requires lower doses and a much shorter duration of treatment.

We have recently reported the antimalarial potential of the human ataxia-telangiectasia mutated (ATM) kinase inhibitor AZD0156 (Figure 1) through inhibition of the clinically validated target *P. falciparum* phosphatidylinositol 4-kinase III*β* (*Pf*PI4K).[13] Like other *Pf*PI4K inhibitors (Figure 1),[14−16] AZD0156 exhibits activity against multiple stages of the *Plasmodium* life cycle (Table 1) and showed efficacy in the *Plasmodium berghei* mouse malaria infection model,[13] making it a promising starting point for antimalarial drug discovery. Toward repositioning AZD0156 for malaria, we present here our first report of structure−activity relationship (SAR) studies based on the imidazo[4,5-*c*]quinolin-2-one core scaffold of AZD0156, leading to several compounds with improved antimalarial activity relative to the parent compound.

Received: May 26, 2025
Revised: July 20, 2025
Accepted: July 30, 2025
Published: August 14, 2025

© 2025 The Authors. Published by American Chemical Society

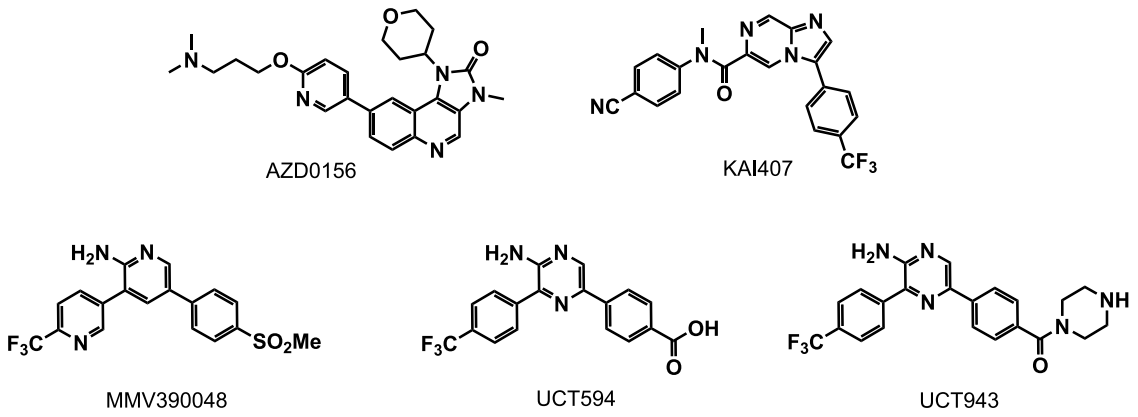

Figure 1. Structure of AZD0156 and examples of other *Pf*PI4K inhibitors.

RESULTS AND DISCUSSION

Chemistry. As previously reported,[17] amination of the 6-bromo-4-chloroquinoline-3-carboxylic acid ethyl ester through nucleophilic displacement of the 4-chloro group with selected amines afforded intermediate **1**, which upon ester hydrolysis under basic conditions gave the quinoline-carboxylic acid derivative **2** (Scheme 1). Curtius rearrangement of **2** with diphenylphosphoryl azide (DPPA) yielded the 8-bromoimidazoquinolines **3**, which was subsequently methylated to generate *N*-methyl-bromoimidazoquinolines **4**. Palladium-catalyzed Suzuki cross-coupling reaction of **4** with either boronic acids or pinacol esters led to the target compounds **8** − **30** (Table 1). Compound **5**, obtained by Suzuki coupling of 6-fluoro-3-pyridinylboronic acid with **4** (R^1 = 4-tetrahydropyran, 4-THP), was reacted with *tert*-butyl 3-hydroxypropylmethylcarbamate and followed by the removal of the *tert*-butyloxycarbonyl group with trifluoroacetic acid to obtain compound **6**. Compound **7** was obtained by Suzuki coupling of **3** (R^1 = 4-THP) with pyridine-3-boronic acid (Scheme 1). The synthesis of key intermediates is provided as Supporting Information.

SAR Exploration Strategies. To identify more potent antimalarial derivatives of AZD0156, we used our published *Pf*PI4K homology model[18] to design compounds able to generate stronger molecular interactions in the *Pf*PI4K active site pocket (Figure 2). As depicted in Figure 2, a hydrogen bond (H-bond) between the quinoline nitrogen of AZD0156 and the hinge amide of V1357 is crucial for ligand binding. Further hydrophobic interactions between the quinoline ring and Y1356 maximize binding. The THP group of AZD0156 extends into the ribose pocket without any apparent polar interactions with S1362. The imidazolinone motif is exposed to the solvent front. The C6 alkoxypyridine extends into the catalytic site of ATP and makes critical H-bond interactions with K1308. The dimethylaminopropyloxy substituent on the C6 pyridine ring is the key structural feature of AZD0156, affording its high potency against the human ortholog *Hs*ATM through H-bond interactions between the terminal amine and a back pocket Y2969 in ATM.[17] However, as this pocket is not accessible in *Pf*PI4K, the amino group of the dimethylaminopropyloxy substituent interacts with D1430. We hypothesized that new derivatives of AZD0156 lacking the dimethylaminopropyloxy substituent would exhibit lower inhibitory activity against *Hs*ATM and potentially be more selective toward the *Plasmodium* enzyme. Similarly, *Pf*PI4K bears a F827 on the phosphate-binding loop, contrary to L374 in the human ortholog, which could be exploited to achieve *Pf*PI4K selectivity through π-stacking interactions.

As summarized in Figure 2, the new analogs maintained the imidazoquinoline core scaffold. Extensive exploration focused on exploiting the catalytic site. The THP group was maintained in most of the new analogues (**5**−**24**, Table 1). The key learnings from the antiplasmodial SAR studies are described below.

Multistage Antiplasmodial Activity. The *in vitro* antiplasmodial activity of the synthesized compounds was assessed against multiple stages of the *P. falciparum* life cycle, including the asexual blood stage (ABS) drug-sensitive (NF54) and multidrug-resistant (K1) strains, immature (>90% stages II−III) and late-stage (>90% stages IV−V) gametocytes (Table 1), as well as liver schizonts, gametes, and oocysts. The compounds were also tested in a *Plasmodium vivax* PI4Kβ (*Pv*PI4K) recombinant enzyme assay to confirm that they maintained PI4K as the primary target, with activity in the low nanomolar range (IC_{50} < 50 nM, Table 1). *Pv*PI4K shares a 97% sequence homology with *Pf*PI4K, sharing similar ATP-binding sites and catalytic regions, and the former can be expressed recombinantly.[18,19] In general, *Pv*PI4K inhibition translated to whole-cell activity against ABS parasites. As expected, there is a general shift in potency between the *Pv*PI4K enzyme and whole-cell IC_{50} values. This can be explained, at least in part, by the high ATP concentrations in the cellular environment relative to the low ATP concentrations used in the enzyme assay. Binding to albumin in the cell culture medium will also reduce the free drug concentration in whole-cell assays in a compound-specific manner.

Asexual Blood-Stage Activity. The removal of the dimethylaminopropyloxy substituent yielded compound **8**, which retained both *Pv*PI4K inhibition (IC_{50} = 0.0060 μM) and ABS activity (IC_{50} *Pf*NF54/*Pf*K1 = 0.090/0.11 μM) comparable to AZD0156. Shortening the dimethylaminopropyloxy substituent to the methoxy in **9** retained *Pv*PI4K activity (IC_{50} = 0.0030 μM), but not *Pf*NF54 (IC_{50} = 0.69 μM). Compound **6** with a methylaminopropyloxy substituent maintained *Pv*PI4K inhibition and *Pf*NF54 activity, slightly more potent than AZD0156. Compound **7**, the *N*-demethylated imidazolinone derivative of **8**, showed comparable *Pv*PI4K inhibition (IC_{50} = 0.0030 μM) and ABS activity (*Pf*IC_{50} = 0.099−0.11 μM) to **8**.

The analogues (**8**−**24**) modified at the C-6 position of the imidazoquinoline core scaffold revealed the significant contributions of these modifications to ABS activity, in some cases regardless of the *Pv*PI4K activity. The SAR suggests that optimal catalytic site interactions (revealed as *Pv*PI4K inhibition) and

https://doi.org/10.1021/acs.jmedchem.5c01417
J. Med. Chem. 2025, 68, 17736−17751

Table 1. *In Vitro Pv*PI4K, Asexual Blood-Stage (ABS), and Gametocytocidal Activities against *P. falciparum*, and Toxicity Evaluation

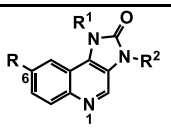

Compound	R	R^1	R^2	*Pv*PI4K IC_{50} (μM)[a]	*Pf* ABS IC_{50} (μM)[b]		*Pf* gametocyte IC_{50} (μM)[c]		CHO, IC_{50} μM[d]	Aq. sol., μM[e]
					NF54	K1	iGC	lGC		
AZD0156	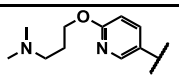		Me	0.0050	0.11	0.20	1.2	1.3	12	195
5	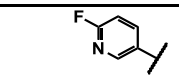		Me	0.019	0.86	0.24	16	3.8	>50	nd
6	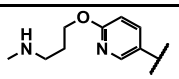		Me	0.0020	0.075	0.11	2.8	0.39	5.0	165
7	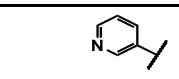		H	0.0030	0.099	0.11	5.6	1.6	7.0	10
8	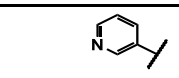		Me	0.0060	0.090	0.11	2.4	0.82	>50	35
9	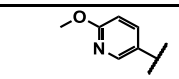		Me	0.0030	0.69	0.12	0.58	0.96	35	nd
10	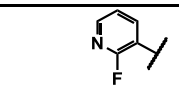		Me	0.0020	0.029	0.066	0.094	0.12	26	20
11	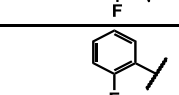	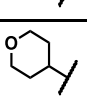	Me	0.021	0.045	0.13	11	2.4	48	<5
12	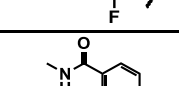		Me	0.0020	0.013	0.032	0.23	0.29	1.0	10
13	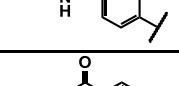		Me	0.029	0.040	0.049	2.0	3.3	>50	10
14	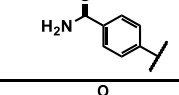		Me	0.050	3.2	3.1	>20	>20	>50	nd
15	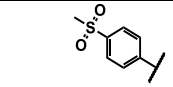		Me	0.031	0.044	0.0029	0.21	0.29	46	<5
16	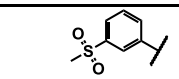		Me	0.020	0.12	0.13	12	5.1	49	nd
17	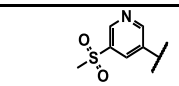		Me	0.0050	0.056	0.037	0.48	0.74	7.0	25
18	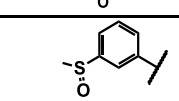		Me	0.0012	0.024	0.053	0.38	0.61	30	195
19	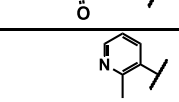	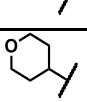	Me	0.028	1.0	1.5	>20	8.4	10	60
20	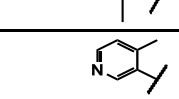	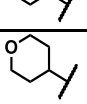	Me	0.0011	0.0084	0.13	0.58	0.031	15	45

https://doi.org/10.1021/acs.jmedchem.5c01417
J. Med. Chem. 2025, 68, 17736−17751

Table 1. continued

Compound	R	R[1]	R[2]	*Pv*PI4K IC_{50} (μM)[a]	*Pf* ABS IC_{50} (μM)[b]		*Pf* gametocyte IC_{50} (μM)[c]		CHO, IC_{50} μM[d]	Aq. sol., μM[e]
					NF54	K1	iGC	lGC		
21	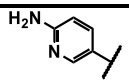		Me	<0.0010	0.011	0.011	0.33	0.13	>50	<5
22	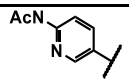		Me	0.0031	0.021	0.035	0.88	0.40	7.0	5
23	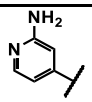		Me	0.0020	0.071	0.053	3.0	1.3	2.0	90
24	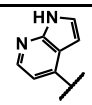		Me	0.0080	0.016	0.20	1.4	0.32	0.90	<5
25	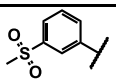		Me	<0.0010	0.0031	0.026	2.3	0.19	>50	190
26	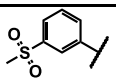		Me	<0.0010	0.0058	0.012	0.58	0.23	6.0	40
27	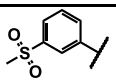		Me	<0.0010	0.022	0.014	1.1	0.51	42	170
28	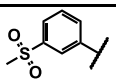		Me	0.0023	0.12	0.079	7.1	3.2	>50	195
29			Me	<0.0010	0.0093	0.012	0.34	0.072	7.0	25
30	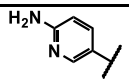		Me	<0.0010	0.0035	0.0027	0.090	0.048	34	<5

nd: Not determined; [a]Inhibition of purified recombinant *Pv*PI4K was determined in the presence of 10 μM ATP and ADP formation was quantified using the ADP-Glo Kinase assay kit; Sapanisertib at a concentration of 10 μM was used as the positive control (*Pv*PI4K IC_{50} = 4 nM). Mean IC_{50} values were calculated based on $n \geq 2$ independent experiments, each with technical duplicates. IC_{50} < 1 nM means below the limit of detection of the assay. [b]IC_{50} values were determined using a SYBR Green I parasite proliferation assay for 96 h, with means calculated from three independent experiments, each with technical triplicates; Chloroquine (*Pf*NF54/*Pf*K1 IC_{50} = 11/143 nM) was used as positive control. [c]Gametocytocidal activity, iGC (immature gametocytes >90% stages II-III), lGC (late-stage gametocytes, >90% stages IV-V) measured by luciferase expression; Methylene blue (iGC/lGC IC_{50} = 190/900 nM) and MMV390048 (iGC/lGC IC_{50} = 215/134 nM) were used as positive controls. Data are from three biological repeats, performed in technical triplicates. [d]Chinese hamster ovary cells tested as one biological replicate with technical triplicates; Emetine (IC_{50} <3 nM) was used as positive control. [e]Thermodynamic Solubility at pH6. *In vitro* data (Mean IC_{50} values ± standard deviation (SD) or standard error (SE)) are provided as Supplementary information file.

consequent ABS activity of this series of analogues are influenced by first, efficient H-bonding with K1308 (Figure 2), which is maximized by the dihedral angle with the quinoline core (as in **5** vs **10**, and **18** vs **19**), and second, an aromatic C-6 group (as in **10** and **11**). That is, **5** (IC_{50} *Pv*PI4K/*Pf*NF54/*Pf*K1 = 0.019/0.86/0.24 μM) showed a marked loss in activity against *Pv*PI4K and ABS relative to its regioisomer **10** (IC_{50} *Pv*PI4K/*Pf*NF54/*Pf*K1 = 0.0020/0.029/0.066 μM). The difference in the activities of **5** and **10** may suggest that a potential twist in the dihedral angle due to the *ortho*-fluoro group in **10** orients the pyridyl N for optimal interactions with K1308, resulting in an improved activity. This hypothesis is corroborated by a similar observation between **18** (IC_{50} *Pv*PI4K/*Pf*NF54/*Pf*K1 = 0.0012/0.024/0.053 μM) and **19** (IC_{50} *Pv*PI4K/*Pf*NF54/*Pf*K1 = 0.028/1.0/1.5 μM). In this case, assuming that the twisting of the dihedral angle by an *ortho* substituent is unidirectional, the pyridyl N in **19** moves further away (opposite phase compared to **18**) from K1308, hence lacked H-bond interaction with loss of activity. In support of this hypothesis, the fluoropyridyl analogue **10** (IC_{50} *Pv*PI4K/*Pf*NF54 = 0.0020/0.029 μM) showed about 10-fold better *Pv*PI4K potency than the fluorophenyl **11** (IC_{50} *Pv*PI4K/*Pf*NF54 = 0.021/0.045 μM), although their ABS activity was within 2-fold. The potent ABS activity of **11** despite the lack of interaction with K1308 highlights the significant contribution of the C-6 aromatic group to whole-cell activity.

Based on these observations, we explored aromatic groups widely reported in *Pf*PI4K inhibitors (*e.g.*, MMV390048 and KDU691) to leverage all possible interactions in the catalytic site for potency. These groups included phenyl amides (**12**, **13**), sulfones (**14**−**16**) and sulfoxides (**17**), aminopyridines (**20**−**23**), and an indole (**24**). The methylamide analogue **12** showed significant improvements in activity (IC_{50} *Pv*PI4K/*Pf*NF54/*Pf*K1 = 0.0020/0.013/0.032 μM) compared to AZD0156. Compound **13** showed marginal (<3-fold) loss in ABS activity and >10-fold loss in *Pv*PI4K potency compared to **12**. The

https://doi.org/10.1021/acs.jmedchem.5c01417
J. Med. Chem. 2025, 68, 17736−17751

Scheme 1. Synthesis of 1,8-Disubstituted Imidazo[4,5-*c*]quinolin-2-one Compounds[a]

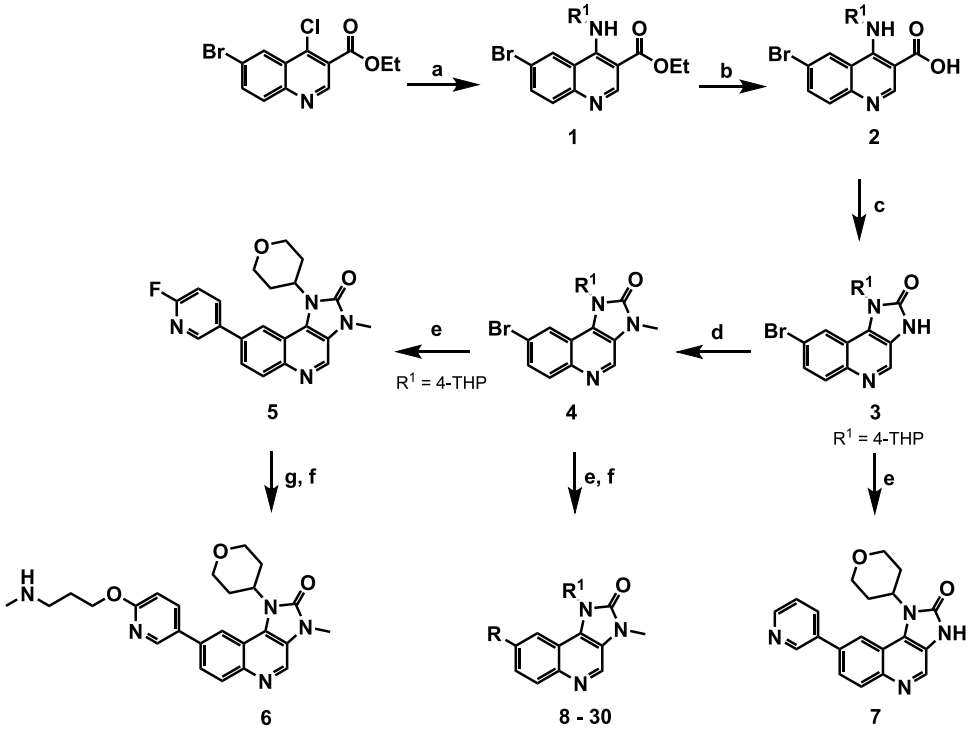

[a]Reagents and reaction conditions: (a) relevant amine, DIPEA or NEt_3, DMF or DMA, 25−90 °C, 3−16 h, 79−87%; (b) NaOH or LiOH, H_2O, MeOH or THF, 25−70 °C, 1−6 h, 75−90%; (c) NEt_3, DPPA, DMF, 60 °C, 0.5−3 h, 74−85%; (d) DMF-DMA, 90 °C, 2 h, 75−92%; (e) boronic acids or pinacol esters, $PdCl_2(PPh_3)_2$, PCy_3, K_2CO_3, DMF/dioxane:H_2O (4:1, *v*/*v*), 100 °C, 1 to 2 h, 68−88%; (f) TFA, DCM, 25 °C, 1 h, 36 − 98% (for **6**, **25**-**28**); (g) *tert*-butyl (3-hydroxypropyl)(methyl)carbamate, NaH (60% dispersion in mineral oil), DMF, 30 °C, 3 h.

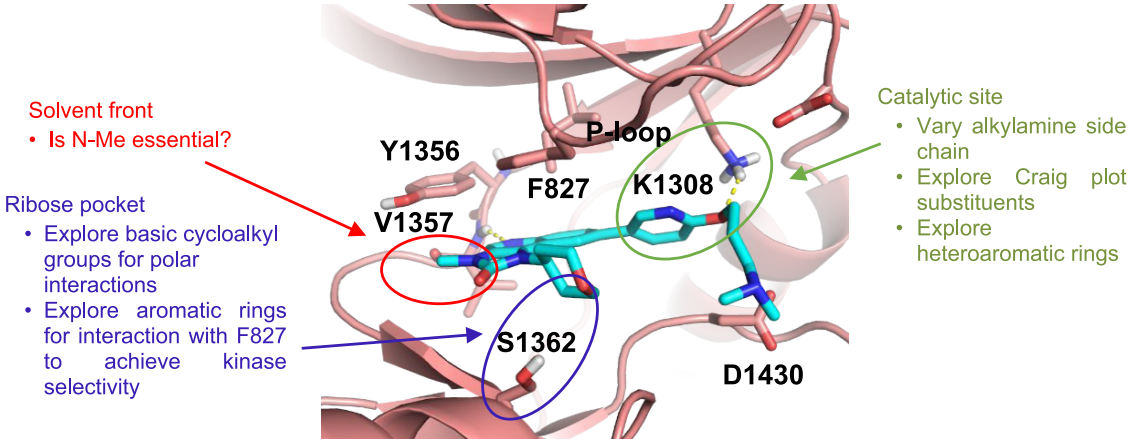

Figure 2. Binding mode of AZD0156 (cyan) in the *Pf*PI4K homology model and SAR exploration strategies. The *Pf*PI4K homology model was built off the human PI4K structure (PDB ID: 4D0L), as previously described.[18]

phenyl amides showed superior activity over the 4-sulfonylphenyl congener **14** (IC_{50} *Pv*PI4K/*Pf*NF54/*Pf*K1 = 0.050/3.2/3.1 μM). However, the 3-sulfonylphenyl regioisomer **15** regained significant ABS potency (IC_{50} *Pv*PI4K/*Pf*NF54/*Pf*K1 = 0.031/0.044/0.0029 μM) comparable to **13**. The combination of the 3-pyridyl and *meta*-sulfonyl group as in **16** (IC_{50} *Pv*PI4K/*Pf*NF54/K1 = 0.020/0.12/0.13 μM) did not potentiate activity. Interestingly, the racemic 3-sulfinylphenyl analogue **17** showed an improvement in *Pv*PI4K inhibition (IC_{50} = 0.0050 μM) compared to the sulfone **15** (IC_{50} = 0.031 μM), indicating stronger interactions of the chiral sulfoxide with K1308 through optimal orientation. All the C-6 aminopyridine analogues (**20**−**23**) retained potent *Pv*PI4K inhibition ($IC_{50} \leq$ 0.0031 μM) and ABS activity (IC_{50} = 0.0084−0.13 μM). The indole derivative **24** showed comparative activity to the aminopyridine congeners.

Replacing the THP group with cycloalkylamines in **25**−**28** while keeping 3-methylsulfonylphenyl at the C-6 position significantly improved *Pv*PI4K inhibition (IC_{50} < 0.0023 μM) and ABS activity ($IC_{50} \leq$ 0.026 μM), as observed for the piperidine analogues (**25**−**27**). These modifications were supported by docking in *Pf*PI4K. Moreover, we envisaged that basic groups would improve the aqueous solubility of these analogs. The most active compounds in our studies were **29** and **30** with *Pv*PI4K activity below the limit of detection of the enzyme assay (IC_{50} < 0.0010 μM), translating to ABS IC_{50}

https://doi.org/10.1021/acs.jmedchem.5c01417
J. Med. Chem. 2025, 68, 17736−17751

values ≤ 0.012 μM in both *Pf*NF54 and K1 strains. These compounds demonstrate the contribution of the π-stacking interactions between the phenyl group and F827 (Figure 2) to *Pf*PI4K potency and ABS activity.

Gametocytocidal Activity. Analyses of the gametocytocidal activities in Table 1 reveal that the compounds were active against either one or both stages of gametocytes. SAR trends above were recapitulated for the gametocytocidal activities of the series, with the activity against late-stage gametocytes directly correlating with *Pv*PI4K inhibition and activity against ABS. Three active compounds (**20**, **29**, and **30**) against *Pv*PI4K (IC_{50} ≤ 0.001 μM) and ABS (IC_{50} < 10 μM) were also the most potent on late-stage gametocytes with IC_{50}'s < 100 μM (lGC = 0.031/0.072/0.048 μM). These dual-stage activities against both ABS and gametocytes have been described for other *Pf*PI4K frontrunner chemotypes.[19] However, as with the majority of other antimalarials, there is still a 4- to 8-fold drop in activity between ABS parasites and late-stage gametocytes as in **20** and **29**, although **30** nears equipotency. Overall, most compounds show <10-fold activity loss toward late-stage gametocytes, a property in line with those from other frontrunner antimalarial candidates, including the known *Pf*PI4K inhibitor MMV390048.[20] With lipoidal uptake seen as the main barrier for dual-stage activity, compounds showing a > 19-fold loss in gametocyte activity could be due to poor compound uptake (i.e., **13**, **16**, **23** and **28** > 75Å tPSA, with a 19- to 83-fold loss in activity, **11** and **19** LogD > 3, with an 8- to 53-fold loss in activity),[20] rather than a difference in target availability between ABS parasites and gametocytes. Interestingly, some compounds (**6** and **8**), aminopyridines (**20**-**23**), indole (**24**), and the THP-modified compounds (**25**-**30**) displayed significant loss in activity to immature gametocytes but not late-stage gametocytes (iGC p = 0.02 compared to ABS, respectively, and lGC p = 0.7 compared to ABS, respectively, two-tailed t test). This is an unusual phenotype that has only been seen for one other *Pf*PI4K targeting compound, UCT943 (IC_{50} *Pf*NF54 = 6.9, iGC = 199, and lGC = 26 nM).[20]

Comparatively, **18** was selected as the best representative compound of the current series for further studies, as detailed below. This compound was potent against *Pv*PI4K, with comparable *Pf*NF54 and *Pf*K1, and gametocytocidal activities. Additionally, **18** possessed a better combination of aqueous solubility and cytotoxicity (Table 1).

Activity against Liver Schizonts, Gametes, and Oocysts. Compound **18** recorded a potent IC_{50} value of 0.065 μM (MMV390048, IC_{50} = 0.046 μM) against *P. falciparum* liver schizonts, which affords it the potential to block the development of schizonts into hypnozoites.[21] These results inspired further studies to investigate the potential of the current compounds to halt the development of sexual parasite forms in the vector stage of the *Plasmodium* life cycle. First, we evaluated the ability of **18** to block transmission using the *P. falciparum* dual gamete formation assay (*Pf*DGFA) in the carry-over format. This assay measures the functional viability of male and female gametocytes and involves the treatment of stage V gametocytes to measure their ability to form gametes.[22] In this assay, the late-stage gametocyte activity of **18** (IC_{50} = 0.61 μM) translated to blocking female gamete formation (IC_{50} = 0.87 μM), albeit to a lesser degree than that against male gamete formation (IC_{50} = 1.5 μM). In related studies, compound **10**, a close analogue of **18**, was 97% effective (at 2 μM) at inhibiting the formation of female gametes from mature gametocytes in the *P. falciparum* female gametocyte activation assay (*Pf*FGAA). Compound **10** recorded comparative activity in the male gamete exflagellation inhibition assay (EIA) by 99% (at 2 μM). Compounds **12** and **15** were equally effective at 100% in the *Pf*FGAA, and 92 and 99% at 2 μM in EIA, respectively.

Lastly, using the standard membrane feeding assay (SMFA) to assess the inhibition of oocyst formation in mosquitoes fed with gametocyte-infected blood, **15** reduced oocyst prevalence by 40% (transmission-blocking activity) and intensity by 69% (transmission-reducing activity). In summary, the current series demonstrates activity against all stages of the *Plasmodium* life cycle.

***Pf*PI4K Is the Primary Target of 18.** We assessed the activity of the current series against field strains of *P. falciparum* and resistant mutant lines raised to compounds in development. In this regard, **17** and **18** showed a <2-fold difference in activity against field isolates relative to the wild-type NF54 strain (Table 2). They were also equally active (<2-fold IC_{50} shift) against laboratory mutants selected by DDD107498,[23] SJ557733,[24] KAF156,[25] and ELQ300[26] relative to the parental *Pf*Dd2 line. Compound **17** showed a 4-fold decrease in activity against the MMV390048-selected *Pf*PI4K S743T[14] mutant, while **18** maintained a marginal 1.9-fold decrease.

Table 2. Activity against Field Isolates and Lab-Raised Resistant Lines of Known Antimalarials[a]

		IC_{50} (μM) (fold shift vs NF54)	
field isolates/strain	resistance profile	**17**	**18**
NF54	Wild type	0.059	0.024
K1	CQ, PYR, CYC, SDOX	0.062 (1.0)	0.053 (2.2)
3D7	Wild type	0.032 (0.5)	0.044 (1.8)
7G8	CQ, CYC, PYR	0.024 (0.4)	0.043 (1.8)
TM90C2B	ATO, CYC, PYR	0.034 (0.6)	0.043 (1.8)
RF12	PPQ	0.024 (0.4)	0.024 (1.0)
Dd2	CQ, CYC, PYR, SDOX	0.035 (0.6)	0.035 (1.4)
lab-raised mutants	mutated locus	IC_{50} (μM) (fold shift vs Dd2)	
Dd2 DDD107498	*Pf*eEF2_Y186N	0.051 (1.4)	0.051 (1.4)
Dd2MMV390048	*Pf*PI4K_S743T	0.15 (4.4)	0.068 (1.9)
Dd2 SJ557733	*Pf*ATP4_G358S	0.039 (1.1)	0.039 (1.1)
Dd2 KAF156	*Pf*CARL_I1139K	0.034 (1.0)	0.034 (1.0)
Dd2 ELQ300	*Pf*CYTB_I22L	0.059 (1.7)	0.059 (1.7)

[a]The fold change in IC_{50} relative to the reference strain is shown in brackets (chloroquine, CQ; Pyrimethamine, PYR; Cycloguanil, CYC; Sulfadoxine, SDOX; Atovaquone, ATO; Piperaquine, PPQ). IC_{50}'s are mean values from at least 2 independent biological replicates using the 72 h [^{3}H]-hypoxanthine incorporation assay. The individual values varied less than 2-fold. Means were calculated from 2 independent experiments each with four technical repeats. RF12 has the additional H97Y mutation in *PfCRT*, which confers PPQ resistance as well as CQ resistance.

To confirm that *Pf*PI4K is the primary target of the current series, we explored the antimalarial resistome barcode sequencing (AReBar) platform[27] for cross-resistance profiling against a pool of over 50 genetically barcoded drug-resistant parasite lines in both the Dd2 and 3D7 background and the two parent lines. The pool, generated using CRISPR/Cas9 genome editing to insert a short barcode cassette into the nonessential *PARE* locus of each parasite line, affords a range of targets and resistance mechanisms to be evaluated (Table S1). Under drug pressure of 3× the Dd2 IC_{50}, the pool exhibited a rapid growth recovery on days 7 and 5 for **17** and **18**, respectively (Figure

https://doi.org/10.1021/acs.jmedchem.5c01417
J. Med. Chem. 2025, 68, 17736−17751

S2a). Both compounds showed a log2 fold change >2.5 for only the *Pf*PI4K S1320L+L1418F mutant parasite line originally selected by KAI407, an imidazopyrazine *Pf*PI4K inhibitor (Figure S2b,c).[16] Clones raised to AZD0156 showed a S1320L mutation in *Pf*PI4K.[13] The *Pf*PI4K S1320L+L1418F mutant showed a significant loss in sensitivity to **17** and **18** relative to the Dd2 line (Figure 3). The *Pf*PI4K S743T+H1484Y mutant line

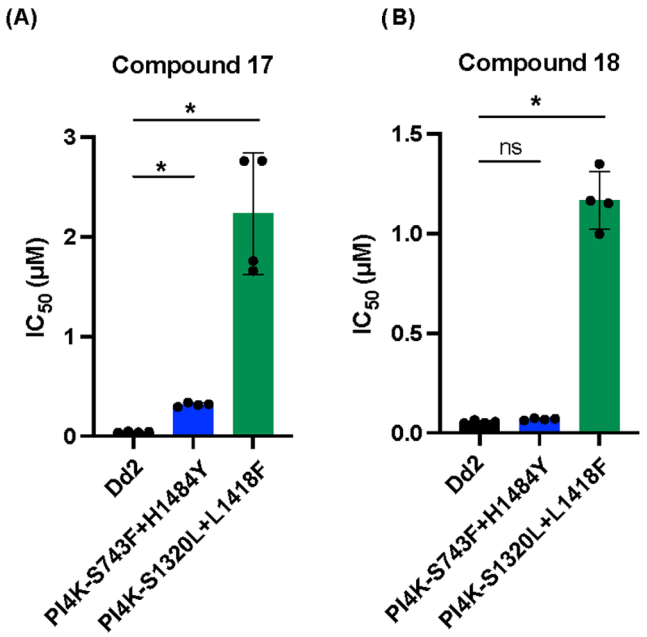

Figure 3. IC_{50} values for (A) **17** and (B) **18** against the parental Dd2 line and the two PI4K mutant lines in the AReBar pool, PI4K−S743F +H1484Y, and PI4K−S1320L+L1418F. EC_{50} data represent means from 4 biological replicates (technical triplicates), with error bars showing standard deviation.

was comparatively more sensitive to the two compounds than the former mutant line. These data support PI4K as the target of **17** and **18** in *Plasmodium*, as is AZD0156.

A major drawback in the development of *Pf*PI4K inhibitors is their propensity to generate resistance arising from mutations in the target, raising concerns about how they will fare in the field. For example, at least nine different *Pf*PI4K single-point mutations within the kinase domain as well as PI4K copy number variations and a single-point mutation in Rab11a have been reported for laboratory-derived resistant lines generated against a range of *Pf*PI4K inhibitors.[14−16,28,29] A recent analysis by researchers in the Malaria Drug Accelerator (MalDA), a consortium aimed to improve and accelerate the early antimalarial drug discovery process by identifying new, essential, druggable targets,[30] classified *Pf*PI4K among deprioritised targets for the reasons above. The propensity for resistance *in vitro* for most *Pf*PI4K inhibitors falls within the moderate range with a minimum inoculum for resistance (MIR) value between 10^6 and 10^7.[14,15]

The MIR of **18** was studied by using the *P. falciparum* Dd2-B2 clone. One MIR single-step selection was set up using 3.3×10^6 Dd2-B2 ABS parasites in 24 wells for a total of 7.9×10^7 parasites, at a starting concentration of $3 \times IC_{90}$ (192 nM). Each well had 2 mL of culture with an initial parasitemia of 1 at 3% hematocrit. Parasite clearance was observed on day 7. The selection had a consistent drug pressure of $3\times IC_{90}$ (192 nM) for 35 days, and cultures were screened three times weekly by flow cytometry and smearing. Wells were considered positive for recrudescence when the overall parasitemia reached 0.3% and parasites were seen on a blood smear. No recrudescence was observed over the course of this selection (MIR > 7.9×10^7). The low propensity for resistance observed for **18**, relative to other *Pf*PI4K inhibitors such as MMV390048 (MIR 10^6−10^7), makes it a promising antimalarial chemotype and provides further evidence that the resistance risk associated with a particular target can vary based on chemotype.[31]

Lastly, like MMV390048 and UCT943 (Figure 1),[14] **17** and **18** displayed a slow parasite reduction ratio (PRR) profile slower than pyrimethamine (log PRR 3.4). Compounds **17** and **18** recorded an *in vitro* log PPR value of 2.4 and 2.6, respectively, comparable to that of MMV390048 (log PRR = 2.7). The parasite clearance time is in the range of 66−69 h (Figure S1). No lag phase was detected for **17**, but a 24 h lag phase was detected for **18**. PRR studies predict how quickly a drug would relieve clinical symptoms as a measure of parasite load. Although slow *in vitro*, MMV390048 showed a moderate rate of kill *in vivo* but a fast-killing profile in the clinic.[29]

Cytotoxicity and hERG. Compound **18** had good safety indices against mammalian cancer cell lines and showed a low human ether-a-go-go-related gene (hERG) cardiotoxicity risk (Table 3). Inhibition of hERG channels may lead to life-threatening cardiac arrhythmias through QT prolongation, which has been associated with many drugs and resulted in their withdrawal from clinical development. Like previous *Pf*PI4K inhibitors, **18** showed potential off-target kinase liabilities based

Table 3. Key Toxicity Profile of Compound 18

	AZD0156	**18**	MMV390048[14,15]
*Pf*NF54/K1, IC_{50}, μM	0.11/0.19	0.024/0.053	0.028/0.025
*Pv*PI4K, IC_{50}, μM @ 10 μM ATP	0.0052	0.0012	0.0010
*Pv*PI4K, IC_{50}, μM @ 500 μM ATP	0.008	0.003	nd
CHO, IC_{50} μM (SI)[a]	12 (109)	30 (1250)	>254 (9071)
HepG2, IC_{50} μM (SI)[a]	4.1% @ 2 μM	18.2 (758)	>100 (3571)
L6, IC_{50} μM (SI)[a]	nd	47.8 (1991)	nd
Vero, IC_{50} μM (SI)[a]	nd	>50 (>2083)	nd
hERG IC_{50}, μM (SI)[a]	>30 (>96)	17.2 (716)	>11 (>393)
*Hs*ATM IC_{50}, μM (SI)[b] @ 10 μM ATP	0.00007 (0.035)	0.002 (2)	nd
*Hs*ATM IC_{50}, μM (SI)[b] @ 500 μM ATP	0.00007 (0.008)	0.103 (34)	nd
*Hs*PI3Kα IC_{50}, μM (SI)[b] @ 10 μM ATP	0.32 (160)	0.53 (530)	7.80 (7800)
*Hs*PI4Kβ IC_{50}, μM (SI)[b] @ 10 μM ATP	1.22 (600)	0.30 (300)	1.00 (1000)
*Hs*MINK1 IC_{50}, μM (SI)[b] @ 10 μM ATP	>10 (>5000)	3.14 (3140)	0.80 (810)
*Hs*MAP4K4 IC_{50}, μM (SI)[b] @ 10 μM ATP	>10 (>5000)	3.17 (3170)	0.70 (740)

[a]Selectivity index (SI = IC_{50}/*Pf*NF54 IC_{50}; [b]SI = IC_{50}/*Pv*PI4K IC_{50}). Mean *Pv*PI4K IC_{50} values were calculated based on two independent experiments where the 10 μM and 500 μM ATP conditions were included in the same assay using the same inhibitor dilution to enable direct comparison. CHO: Chinese Hamster Ovary cells; HepG2: Human hepatoblastoma cell line; L6: Rat myoblast cell line; Vero: Monkey kidney epithelial cells; hERG: Human ether-a-go-go-related gene; *Hs*MINK1: human misshapen-like kinase 1; *Hs*MAP4K4: human mitogen-activated protein kinase 4; nd: Not determined.

https://doi.org/10.1021/acs.jmedchem.5c01417
J. Med. Chem. 2025, 68, 17736−17751

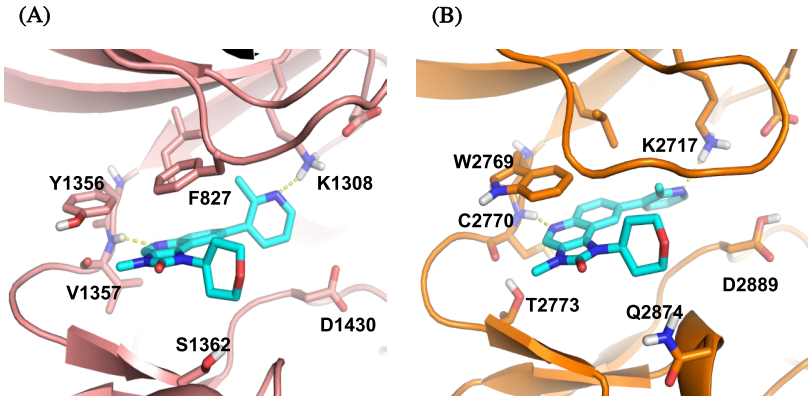

Figure 4. Binding mode of **18** in (A) *Pf*PI4K homology model and (B) *Hs*ATM. The *Pf*PI4K homology model was built off the human PI4K structure (PDB ID: 4D0L), as previously described.[18] The *Hs*ATM crystal structure (PDB ID 7NI4) was used.[34]

on *in vitro* human kinase inhibition data for a small panel of key kinase off-targets as described below (Table 3).

Human Kinase Profiles. *Compound **18** and the PIKKs.* AZD0156 shows significant selectivity toward *Hs*ATM compared to other members (such as ATR, DNA-PK, mTOR)[17] of the phosphatidylinositol 3-kinase-related kinase (PIKK) family. Although the PIKKs are a family of serine/threonine kinases, as the name suggests, they are structurally similar to the phosphatidylinositol 3-kinases (PI3Ks).[32] Hence, we tested AZD0156 and **18** against both *Hs*ATM and *Hs*PI3Kα to gain insight into the kinase selectivity. Like AZD0156, **18** showed moderate inhibition of *Hs*PI3Kα, with good selectivity for *Pv*PI4K. Although compound **18** retained potency against *Hs*ATM (IC_{50} = 2 nM), a 30-fold reduction in potency was observed relative to that of AZD0156 (IC_{50} = 0.07 nM).

Given the marked difference in the ATP Michaelis constant (K_m^{ATP}) values for *Pv*PI4K (K_m^{ATP} = 300 μM) and *Hs*ATM (K_m^{ATP} = 10 μM), we investigated the activity of **18** at a higher ATP concentration in both the *Pv*PI4K and *Hs*ATM biochemical assays. Under these conditions, the *Pv*PI4K IC_{50} values for **18** and AZD0156 at 10 and 500 μM were within 2- to 4-fold, in line with what is expected based on the Cheng−Prusoff equation ($K_i = IC_{50}/(1 + [S]/K_m)$, where K_i is the inhibition constant, and [S] is the ATP concentration). AZD0156, which has been reported to retain subnanomolar potency in a cell-based ATM inhibition assay,[17] displayed an *Hs*ATM IC_{50} value of 0.07 nM in the presence of both 10 μM and 500 μM ATP. This is most likely because the IC_{50} value for AZD0156 is at the lower limit of detection of the *in vitro* enzyme assay, so the expected increase in IC_{50} at higher ATP concentration is not observed. In contrast, **18** showed ∼50-fold higher IC_{50} (*Hs*ATM IC_{50} = 103 nM) at 500 μM ATP than at 10 μM ATP (*Hs*ATM IC_{50} = 2 nM), as expected based on the Cheng−Prusoff equation. Compared to AZD0156, **18** is only ∼28-fold less potent against *Hs*ATM at 10 μM ATP (AZD0156/**18** IC_{50} = 0.07/2 nM), but ∼ 1470-fold less potent against *Hs*ATM at 500 μM ATP (AZD0156/**18** IC_{50} = 0.07/103 nM). We hypothesize that **18** would show much lower *Hs*ATM inhibitory activity under cellular conditions where the ATP concentration is much higher than 500 μM.[33] In contrast, the shift in IC_{50} for *Pv*PI4K is expected to be lower due to the higher K_m^{ATP}.

In Figure 4, **18** shows similar interactions with the amino acid residues in the ATP-binding site of *Pf*PI4K and *Hs*ATM. However, subtle differences could be explored to achieve selectivity. For example, *Pf*PI4K has a small S1362 compared to a larger Q2874 of *Hs*ATM. New analogues designed to incorporate bulky groups extending into the ribose pocket could disrupt binding in *Hs*ATM but could be accommodated in *Pf*PI4K, thereby achieving selectivity at the enzyme level.

*Compound **18** and HsPI4K, MINK1, and MAP4K4.* A recent study on MMV390048 hypothesized a potential link between the inhibition of *Hs*PI4K and *Hs*MINK1 and/or *Hs*MAP4K4 and the *in vivo* malformations observed in embryofetal developmental studies in rats (but not rabbits).[35] Compound **18** showed ∼4-fold reduction in potency for *Hs*MINK1 and *Hs*MAP4K4, relative to MMV390048, while AZD0156 was inactive (IC_{50} > 10 μM, Table 3). AZD0156 and MMV390048 showed comparable inhibition of *Hs*PI4K (IC_{50} ∼ 1 μM), while **18** was ∼3-fold more potent, highlighting the need to improve the selectivity of future congeners in relation to *Hs*PI4K. *Plasmodium* and human PI4K have similar ATP-binding sites and K_m values. As described for *Hs*ATM (Figure 4), it has been speculated that the selectivity of MMV390048 over *Hs*PI4K is due to a clash between the pyridyl-CF_3 group and the bulky ribose pocket Q606 residue.[18] These hypotheses (that is, exploring bulky groups predicted to extend into the ribose pocket of the *Hs*PI4K and *Hs*ATM ATP-binding sites and testing the analogues in a cell-based *Hs*ATM assay) are the subject of ongoing work in our laboratories.

***In Vitro* and *In Vivo* DMPK.** Compound **18** showed an excellent *in vitro* ADME profile to support *in vivo* pharmacokinetic studies in rodents (mouse and rat) (Table 4). Consistent with the *in vitro* data, the unbound clearance of **18** was low across the species. Further to this, **18** showed significantly lower unbound clearance in mice compared to AZD0156. The low unbound clearance of **18** resulted in higher free drug concentration relative to AZD0156 (free AUC = 380.9 and 42.7 min.μmol/L for **18** and AZD0156, respectively, in mouse at a 10 mg/kg oral dose). Absorption was complete (bioavailability = 100%) in rats but lower in mice (55%) due to the lower unbound clearance in rats compared to mice.

***In Vivo* Efficacy of 18.** Compound **18** was tested in a humanized NOD-*scid IL-2Rγnull* (NSG) mouse model of malaria by administering quadruple ascending oral doses of 1, 3, 10, and 30 mg kg^{-1} 3 days postinfection. These quadruple doses were administered 24 h apart. The blood samples from treated mice were screened for drug concentration and parasitemia every 24 h from day 3 until day 7 post-treatment to generate the pharmacokinetic and pharmacodynamic parameters (Figure 5). The compound showed an ED_{90}, the effective dose in mg kg^{-1} that reduces parasitemia by 90% on day 7 postinfection compared to the untreated control group, of 4.6

https://doi.org/10.1021/acs.jmedchem.5c01417
J. Med. Chem. 2025, 68, 17736−17751

Table 4. *In Vitro* and *In Vivo* DMPK Parameters[a]

compound	AZD0156	**18**
NF54/K1, IC_{50}, μM	0.11/0.19	0.024/0.053
solubility PBS pH 6.5 (μM)/LogD/tPSA	195/1.26/71	195/2.45/58
PAMPA Papp (10^{-6} cm/s)	20	340
Caco-2 Papp A > B (10^{-6} cm/s)	nd	23
efflux ratio	nd	1
PPB fu h/m	0.22/0.05	0.12/0.42
microsomal CL_{int}, app h/r/m (mL/min/kg)	<10/<21/<46	<10/<21/<46
hepatocyte CL_{int}, app h/r (mL/min/kg)	<15/nd	<15/<30
in vivo mouse CL_b/CL_u (mL/min/kg)	15.3/306	16.3/38.8
in vivo rat CL_b/CL_u (mL/min/kg)	nd	4.6/10.9
$t_{1/2}$ terminal r/m (h)	nd/4.1	4.1/9.0
$V_{ss}/V_{ss,u}$ mouse (L/kg)	3.5/70	3.9/9
$V_{ss}/V_{ss,u}$ rat (L/kg)	nd	1.8/4
AUC_{0-t} r/m (min.μM)	nd/853	7172/907
F r/m (%)	nd/50	100/55
F_{abs} r/m	nd/0.56	1.0/0.63

[a]*In vivo* mouse PK parameters calculated from noncompartmental analysis of intravenous dosing at 3 mg kg^{-1}; tPSA: total polar surface area; h/r/m: Human/Rat/Mouse; PPB: Plasma protein binding; fu: Fraction unbound; Vss: Apparent volume of distribution at steady state; Vss,u: Unbound apparent volume of distribution at steady state; CL_b: Total body clearance determined from whole blood; CL_u: Unbound blood clearance determined from CL_b and plasma protein binding (assuming blood to plasma ratio of 1). AUC: Area under the curve; not determined (nd).

mg kg^{-1} with the corresponding oral exposure levels (AUC_{ED90}) of 22.7 μM.hr.

CONCLUSIONS

New affordable antimalarial drugs with a low propensity for resistance are needed to circumvent the rapid rise in resistance toward ACTs. In addition, blocking transmission of *Plasmodium* parasites from humans to mosquitoes is essential for malaria elimination as set out in the World Health Organization Global Technical Strategy for Malaria 2016−2030.[36] Therefore, developing drugs that can target the *Plasmodium* parasites at the asexual blood stage to ease symptoms and block human-to-mosquito transmission is critical for malaria control and elimination. The AZD0156-based PI4K inhibitors described in this study show the potential for further optimization to identify clinical candidates that would be effective against both asexual and sexual life stages of malaria in achieving this goal. In this regard, further work is ongoing to improve the antimalarial potential of **18** with a special focus on improving the selectivity relative to the human ATM, PI3, and PI4 kinases.

EXPERIMENTAL SECTION

Modeling. All docking simulations were run on the *Pf*PI4K homology model[18] or structures downloaded from the PDB. Protein structures were all processed using the Maestro GUI of the Schrodinger 2023−4 (Schrödinger Release 2023−4: Schrödinger, LLC, New York, NY, 2023) software suite. Protein structures were prepared using the Schrodinger Protein Preparation wizard using default preprocessing, H-bond optimization, and minimization settings. Crystallization artifacts were manually removed, and residues with alternate positions were manually assigned. The prepared ligand binding site was then visually inspected for the correct tautomer and H-bond assignment.

Docking grids were then prepared using the GLIDE Receptor Grid Generation tool with a grid centered upon previously docked ligands in the active site or the crystallized ligand from *Hs*PI4K.[37] A hydrogen bonding constraint on the hinge H-bond donating amide (*Pf*PI4K V1357, *Hs*PI4K V598, *Hs*ATM C2770) was also set. All ligands were prepared from SMILES using LigPrep with ionization states determined to a pH of 7 ± 1.0, calculated using the Epik and the OPLS4 atomic force field.[38] The prepared ligands were then docked into the prepared docking grids by using SP docking. All docking images were generated using open source PyMOL 2.5.0 (Schrodinger, LLC. 2010. The PyMOL Molecular Graphics System, Version 2.5.0).

Chemistry. All commercially available chemicals were purchased from Sigma-Aldrich, Merck, or Combi-Blocks Limited and were of >95% purity, thus generally used without further purification. Reactions were monitored with LCMS. Compounds were purified on silica gel chromatography using flash column chromatography on a Biotage Isolera One system (Biotage AB, Uppsala, Sweden). ^{1}H NMR spectra were recorded on a Varian Mercury (300 MHz) or Bruker (600 MHz). ^{13}C NMR spectra were recorded on the Bruker Ultrashield-Plus (101 MHz) or a Bruker (151 MHz). NMR samples were dissolved in deuterated dimethyl sulfoxide (DMSO-d_6), chloroform ($CDCl_3$), or methanol (CD_3OD). Chemical shifts (δ) are reported in parts per million (ppm) and rounded to two decimal places. Coupling constants (J) are reported in hertz (Hz) and rounded to two decimal places. Abbreviations used in assigning ^{1}H NMR signals are d (doublet), dd (doublet of doublets), ddd (doublet of doublets of doublets), m

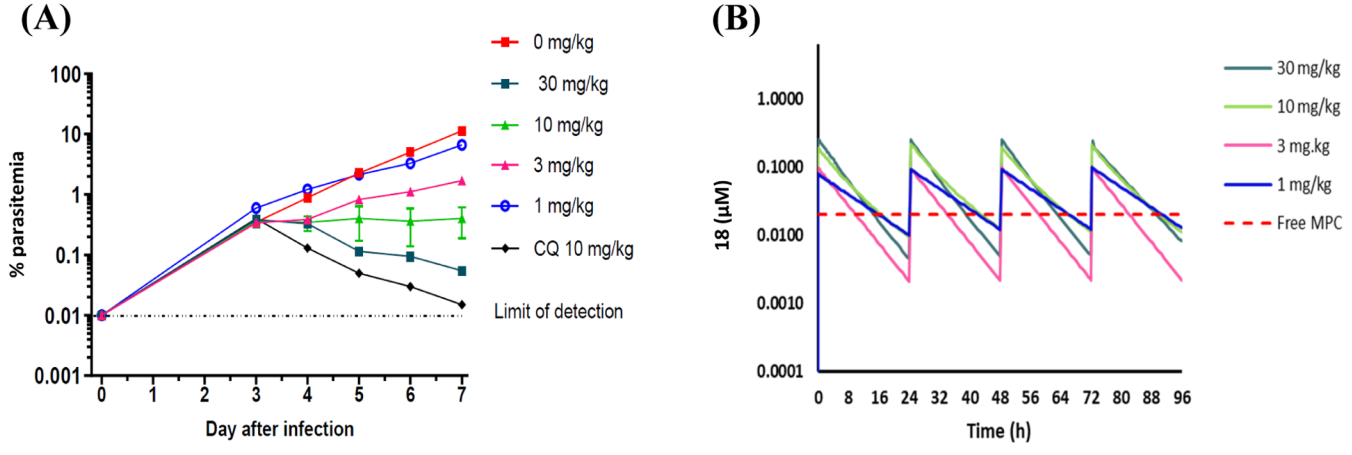

Figure 5. (A) *In vivo* therapeutic efficacy of **18** in the humanized NSG mice infected with *P. falciparum Pf*3D7$^{0087/N9}$ cells and (B) the free plasma concentrations vs time in NSG mice following a quadruple dose regimen. The red dashed line represents the free *in vitro* minimum parasiticidal concentration (MPC) of compound **18**.

https://doi.org/10.1021/acs.jmedchem.5c01417
J. Med. Chem. 2025, 68, 17736−17751

(multiplet), q (quartet), s (singlet), t (triplet), and td (triplet of doublets).

Purity was determined using an Agilent 1260 Infinity binary pump, Agilent 1260 Infinity diode array detector (DAD), Agilent 1290 Infinity column compartment, Agilent 1260 Infinity standard autosampler, and Agilent 6120 quadrupole (single) mass spectrometer equipped with an ESI ionization source. LC purity analyses were performed using a Kinetex 1.7 μM C18 reverse phase column, 1 μL injection volume, flow 1.2 mL/min; gradient: 5−100% B in 1.5 min (hold 0.4 min), 100−5% in 0.3 min (hold 0.5 min) (Mobile phase A: 0.1% formic acid in H_2O and Mobile phase B: 0.1% formic acid in acetonitrile). The diode array detector was programmed to scan the eluents at an absorption wavelength range of 210−640 nm. All synthesized intermediates were characterized by LCMS, while final compounds were confirmed by LCMS and, at least, ^{1}H NMR data. All compounds tested for biological activity were confirmed to have >95% purity. Intermediates **2**−**4** were synthesized as previously described.[17]

General Synthesis Methods. Method A: 8-Bromo-3-methyl-1-(tetrahydro-2*H*-pyran-4-yl)-1,3-dihydro-2*H*-imidazo[4,5-*c*]quinolin-2-one **4** (0.100 g, 0.28 mmol), the appropriate boronic acid/boronic acid pinacol ester (1.50 equiv), $PdCl_2(PPh_3)_2$ (0.007 g, 0.01 mmol), PCy_3 (0.008 mg, 0.03 mmol), and K_2CO_3 (0.057 g, 0.41 mmol) were placed in a round-bottom flask equipped with a stirrer bar and a condenser. DMF/dioxane/water (4:1 *v*/*v*, 75 mL/mmol of **4**) was added, and the mixture was purged with nitrogen gas for 10 min. A balloon filled with nitrogen gas was connected to the top of the condenser, and the mixture was stirred at 100 °C for 2 h or until the reaction was complete (LCMS monitored). After the completion of the reaction, the mixture was cooled to ambient temperature and then quenched with ice-cold water. The precipitate formed was obtained by filtration, dissolved in DCM (50 mL), and washed with brine (2 × 20 mL). The organic layer was dried over anhydrous $MgSO_4$ and was filtered through Celite. The solvent was evaporated under reduced pressure on a rotary evaporator. The crude product was adsorbed onto silica gel and purified by flash column chromatography, eluting with a gradient of ethyl acetate in petroleum ether, unless otherwise stated. Fractions containing the desired compound were evaporated to dryness to afford the target compounds.

Method B: Boc-protected compound was dissolved in a DCM:TFA mixture (15 mL, 2:1 *v*/*v*). The mixture was stirred at 25 °C for 1 h, and then the solvent was removed under reduced pressure (LCMS monitored). The crude product was purified by reverse phase chromatography (C18 OBD column, 5 μm silica, 19 mm diameter, 150 mm length), using decreasingly polar mixtures of Milli-Q water and MeOH as eluents. Fractions containing the desired compound were evaporated to dryness to afford pure product **6**.

*8-(6-Fluoropyridin-3-yl)-3-methyl-1-(tetrahydro-2H-pyran-4-yl)-1,3-dihydro-2H-imidazo[4,5-c]quinolin-2-one (**5**).* Synthesized from **4** (0.100 g, 0.28 mmol) and 6-fluoro-3-pyridinylboronic acid (0.058 g, 0.41 mmol), according to Method A to give **5** as a yellow solid (0.085 g, 82% yield); ^{1}H NMR (300 MHz, $CDCl_3$) δ 8.78 (s, 1H), 8.61 (s, 1H), 8.51 (s, 1H), 8.32 (d, J = 8.8 Hz, 1H), 8.30−8.14 (m, 1H), 7.85 (d, J = 8.8 Hz, 1H), 7.14 (dd, J = 8.5, 3.1 Hz, 1H), 5.17−5.09 (m, 1H), 4.30−4.24 (m, 2H), 3.67−3.58 (m, 5H), 3.04−2.80 (m, 2H), 2.01−1.94 (m, 2H). LC-MS: t_R = 0.763 min (Purity = 98%); m/z = 379.1 $[M + H]^+$ (anal. calcd. for $C_{21}H_{19}FN_4O_2$: m/z = 378.1).

*3-Methyl-8-(6-(3-(methylamino)propoxy)pyridin-3-yl)-1-(tetrahydro-2H-pyran-4-yl)-1,3-dihydro-2H-imidazo[4,5-c]quinolin-2-one (**6**).* Following Method B, *tert*-butyl methyl(3-((5-(3-methyl-2-oxo-1-(tetrahydro-2*H*-pyran-4-yl)-2,3-dihydro-1*H*-imidazo[4,5-*c*]-quinolin-8-yl)pyridin-2-yl)oxy)propyl)carbamate (0.10 g; 0.18 mmol) in DCM:TFA (15 mL) afforded **6** as a white solid (0.05 g, 62% yield); ^{1}H NMR (300 MHz, DMSO-d_6) δ 9.14 (s, 1H), 8.72 (s, 1H), 8.66−8.39 (m, 2H), 8.52 (s, 1H), 8.27 (d, J = 8.8 Hz, 1H), 8.16 (d, J = 8.8 Hz, 1H), 7.05 (d, J = 8.9 Hz, 1H), 5.24−5.13 (m, 1H), 4.43 (t, J = 6.1 Hz, 2H), 4.09−4.06 (m, 2H), 3.64−3.55 (m, 5H), 2.74−2.71 (m, 2H), 2.62 (s, 3H), 2.54−2.48 (m, 2H), 2.10 (t, J = 7.2 Hz, 2H), 1.99−1.95 (m, 2H) ^{13}C NMR (101 MHz, $CDCl_3$) δ 163.57, 162.83, 162.48, 153.43, 145.16, 137.76, 136.85, 131.85, 129.16, 129.03, 128.66, 127.64, 123.75, 115.20, 111.82, 67.53 (2C), 62.91, 46.76, 33.14, 29.97 (2C), 29.72, 27.86, 25.93. LC-MS: t_R = 0.596 min (Purity = 98%); m/z = 448.2 $[M + H]^+$ (anal. calcd. for $C_{25}H_{29}N_5O_3$: m/z = 447.2).

*8-(Pyridin-3-yl)-1-(tetrahydro-2H-pyran-4-yl)-1,3-dihydro-2H-imidazo[4,5-c]quinolin-2-one (**7**).* Synthesized from 8-bromo-1-(tetrahydro-2*H*-pyran-4-yl)-1,3-dihydro-2*H*-imidazo[4,5-*c*]quinolin-2-one **3** (0.120 g, 0.34 mmol) and 3-(4,4,5,5-tetramethyl-1,3,2-dioxaborolan-2-yl)pyridine (0.106 g, 0.52 mmol) according to Method A to give **7** as a beige solid (0.023 g, 19% yield); ^{1}H NMR (300 MHz, DMSO-d_6) δ 11.59 (s, 1H), 9.09 (s, 1H), 8.72−8.61 (m, 2H), 8.51 (s, 1H), 8.27 (d, J = 8.0 Hz, 1H), 8.15 (d, J = 8.8 Hz, 1H), 8.00 (d, J = 8.8 Hz, 1H), 7.87−7.16 (m, 1H), 5.11 (s, 1H), 4.12−3.99 (m, 2H), 3.58 (t, J = 11.9 Hz, 2H), 2.83−2.65 (m, 2H), 2.02−1.88 (m, 2H). LC-MS: t_R = 0.536 min (Purity = 100%); m/z = 347.1 $[M + H]^+$ (anal. calcd. for $C_{20}H_{18}N_4O_2$: m/z = 346.1).

*3-Methyl-8-(pyridin-3-yl)-1-(tetrahydro-2H-pyran-4-yl)-1,3-dihydro-2H-imidazo[4,5-c]quinolin-2-one (**8**).* Synthesized from **4** (0.125 g, 0.34 mmol) and 3-(4,4,5,5-tetramethyl-1,3,2-dioxaborolan-2-yl)-pyridine (0.106 g, 0.52 mmol) according to Method A to afford **8** as a beige solid (0.056g, 45% yield); ^{1}H NMR (300 MHz, DMSO-d_6) δ 9.09 (s, 1H), 8.92 (s, 1H), 8.69−8.61 (m, 1H), 8.51 (s, 1H), 8.27 (d, J = 8.0 Hz, 1H), 8.17 (d, J = 8.8 Hz, 1H), 8.00 (d, J = 8.9 Hz, 1H), 7.59 (t, J = 6.3 Hz, 1H), 5.17 (d, J = 12.6 Hz, 1H), 4.12−4.01 (m, 2H), 3.66−3.53 (m, 2H), 3.52 (s, 3H), 2.86−2.62 (m, 2H), 1.93 (d, J = 12.8 Hz, 2H). LC-MS: t_R = 0.590 min (Purity = 100%); m/z = 361.2 $[M + H]^+$ (anal. calcd. for $C_{21}H_{20}N_4O_2$: m/z = 360.2).

*8-(6-Methoxypyridin-3-yl)-3-methyl-1-(tetrahydro-2H-pyran-4-yl)-1,3-dihydro-2H-imidazo[4,5-c]quinolin-2-one (**9**).* Synthesized from **4** (0.100 g, 0.28 mmol) and 2-methoxypyridine-5-boronic acid (0.063 g, 0.41 mmol) according to Method A to give **9** as a white solid (0.057 g, 53% yield); ^{1}H NMR (600 MHz, DMSO-d_6) δ 8.88 (s, 1H), 8.67 (d, J = 2.6 Hz, 1H), 8.43 (m, 1H), 8.18 (dd, J = 8.6, 2.6 Hz, 1H), 8.14 (d, J = 8.8 Hz, 1H), 7.96−7.92 (m, 1H), 7.00 (d, J = 8.7 Hz, 1H), 5.18−5.09 (m, 1H), 4.08 (dd, J = 11.6, 4.6 Hz, 2H), 3.96 (s, 3H), 3.63−3.56 (m, 2H), 3.52 (s, 3H), 2.74 (m, 2H), 1.96−1.90 (m, 2H). ^{13}C NMR (151 MHz, DMSO-d_6) δ 163.26, 152.76, 145.04, 143.78, 137.67, 134.52, 133.06, 131.25, 128.78, 127.87, 125.04, 123.13, 117.99, 115.14, 110.64, 66.53 (2C), 53.19, 52.67, 29.62 (2C), 26.98. LC-MS: t_R = 0.787 min (Purity = 97%); m/z = 391.2 $[M + H]^+$ (anal. calcd. for $C_{22}H_{22}N_4O_3$: m/z = 390.2).

*8-(2-Fluoropyridin-3-yl)-3-methyl-1-(tetrahydro-2H-pyran-4-yl)-1,3-dihydro-2H-imidazo[4,5-c]quinolin-2-one (**10**).* Synthesized from **4** (0.100 g, 0.28 mmol) and 2-fluoropyridine-3-boronic acid (0.059 g, 0.41 mmol) according to Method A to give **10** as a white solid (0.077 g, 74% yield); ^{1}H NMR (600 MHz, DMSO-d_6) δ 8.93 (s, 1H), 8.57 (m, 1H), 8.35 (m, 1H), 8.31 (m, 1H), 8.18 (d, J = 8.8 Hz, 1H), 7.89 (m, 1H), 7.57 (m, 1H), 5.08 (m, 1H), 4.05 (m, 2H), 3.59−3.48 (m, 5H), 2.72 (m, 2H), 1.94−1.88 (m, 2H). ^{13}C NMR (151 MHz, DMSO-d_6) δ 159.67 (d, J = 237.2 Hz), 152.74, 146.56 (d, J = 15.2 Hz), 143.91, 141.34 (d, J = 3.8 Hz), 133.72, 130.90, 130.67 (d, J = 5.3 Hz), 128.05, 126.47, 123.18, 122.69 (d, J = 4.1 Hz), 122.45, 122.27, 114.71, 66.45 (2C), 52.97, 29.58 (2C), 26.99. LC-MS: t_R = 0.750 min (Purity = 96%); m/z = 379.2 $[M + H]^+$ (anal. calcd. for $C_{21}H_{19}FN_4O_2$: m/z = 378.1).

*8-(2-Fluorophenyl)-3-methyl-1-(tetrahydro-2H-pyran-4-yl)-1,3-dihydro-2H-imidazo[4,5-c]quinolin-2-one (**11**).* Synthesized from **4** (0.100 g, 0.28 mmol) and 2-fluorophenylboronic acid (0.058g, 0.41 mmol) according to Method A to give **11** as a white solid (0.085 g, 82% yield); ^{1}H NMR (600 MHz, DMSO-d_6) δ 8.92 (s, 1H), 8.51 (m, 1H), 8.15 (d, J = 8.8 Hz, 1H), 7.87−7.82 (m, 1H), 7.81−7.75 (m, 1H), 7.67−7.59 (m, 1H), 7.59−7.47 (m, 2H), 7.42−7.37 (m, 2H), 5.06 (m, 1H), 4.05 (m, 2H), 3.55−3.48 (m, 5H), 2.76−2.66 (m, 2H), 1.90 (m, 2H). ^{13}C NMR (151 MHz, DMSO-d_6) δ 159.41 (d, J = 246.5 Hz), 152.82, 143.82, 133.63, 132.44, 131.97, 131.43 (d, J = 9.5 Hz), 130.00 (d, J = 8.6 Hz), 128.69 (d, J = 11.6 Hz), 128.07, 127.55 (d, J = 12.3 Hz), 127.01, 126.99, 125.22, 123.17, 116.40 (d, J = 22.6 Hz), 114.86, 66.64 (2C), 53.67, 29.74 (2C), 27.13. LC-MS: t_R = 0.853 min (Purity = 100%); m/z = 378.2 $[M + H]^+$ (anal. calcd. for $C_{22}H_{20}FN_3O_2$: m/z = 377.2).

*N-Methyl-4-(3-methyl-2-oxo-1-(tetrahydro-2H-pyran-4-yl)-2,3-dihydro-1H-imidazo[4,5-c]quinolin-8-yl)benzamide (**12**).* Synthe-

https://doi.org/10.1021/acs.jmedchem.5c01417
J. Med. Chem. 2025, 68, 17736−17751

sized from **4** (0.100 g, 0.28 mmol) and (4-(methylcarbamoyl)phenyl)-boronic acid (0.074 g, 0.41 mmol) according to Method A to give **12** as a white solid (0.083 g, 73% yield); ^{1}H NMR (300 MHz, DMSO-d_6) δ 8.92 (s, 1H), 8.58−8.49 (m, 2H), 8.17 (d, J = 8.9 Hz, 1H), 8.07−7.89 (m, 5H), 5.28−5.04 (m, 1H), 4.12−4.05 (m, 2H), 3.67−3.47 (m, 5H), 2.83 (s, 3H), 2.82−2.64 (m, 2H), 1.97−1.92 (m, 2H). ^{13}C NMR (151 MHz, DMSO-d_6) δ: 166.73, 153.47, 142.51, 137.34, 134.40, 133.90, 131.84, 128.41 (2C), 128.19, 127.33 (2C), 127.08, 125.91, 123.88, 119.74, 115.73, 67.26 (2C), 40.76, 30.34 (2C), 27.66, 26.67. LC-MS: t_R = 0.710 min (Purity = 97%); m/z = 417.2 $[M + H]^+$ (anal. calcd. for $C_{24}H_{24}N_4O_3$: m/z = 416.2).

*4-(3-Methyl-2-oxo-1-(tetrahydro-2H-pyran-4-yl)-2,3-dihydro-1H-imidazo[4,5-c]quinolin-8-yl)benzamide (**13**).* Synthesized from **4** (0.100 g, 0.28 mmol) and (4-carbamoylphenyl)boronic acid (0.068 g, 0.41 mmol) according to Method A to give **13** as a white solid (0.077 g, 70% yield); ^{1}H NMR (300 MHz, DMSO-d_6) δ 8.93 (s, 1H), 8.54 (s, 1H), 8.17 (d, J = 8.9 Hz, 1H), 8.11−8.02 (m, 3H), 7.96 (d, J = 8.4 Hz, 2H), 7.48 (br.s 2H), 5.30−5.00 (m, 1H), 4.11−4.06 (m, 2H), 3.65−3.49 (m, 5H), 2.80−2.66 (m, 2H), 2.02−1.89 (m, 2H). ^{13}C NMR (151 MHz, DMSO-d_6) δ: 167.98, 153.47, 142.29, 137.37, 134.21, 133.95, 131.89, 128.84 (2C), 128.62 (2C), 127.29 (2C), 127.06 (2C), 125.92, 67.27 (2C), 30.35 (2C), 27.65 (2C). LC-MS: t_R = 0.675 min (Purity = 98%); m/z = 403.2 $[M + H]^+$ (anal. calcd. for $C_{23}H_{22}N_4O_3$; m/z = 402.2).

*3-Methyl-8-(4-(methylsulfonyl)phenyl)-1-(tetrahydro-2H-pyran-4-yl)-1,3-dihydro-2H-imidazo[4,5-c]quinolin-2-one (**14**).* Synthesized from **4** (0.100 g, 0.28 mmol) and (4-(methylsulfonyl)phenyl)-boronic acid (0.082 g, 0.41 mmol) according to Method A to give compound **14** as a yellow solid (0.082 g, 73% yield); ^{1}H NMR (300 MHz, DMSO-d_6) δ 8.95 (s, 1H), 8.56 (s, 1H), 8.24−7.99 (m, 6H), 5.32−4.99 (m, 1H), 4.10−4.05 (m, 2H), 3.55−3.61 (m, 2H), 3.53 (s, 3H), 3.32 (s, 3H), 2.83−2.63 (m, 2H), 1.96−1.92 (m, 2H). ^{13}C NMR (101 MHz, DMSO-d_6) δ: 154.30, 147.39, 142.69, 142.12, 137.99, 136.01, 130.96, 128.68, 129.00 (2C), 127.02, 126.83, 124.98 (2C), 121.19, 116.01, 67.19 (2C), 44.52, 30.11 (2C), 28.14 (2C). LC-MS: t_R = 0.744 min (Purity = 97%); m/z = 438.1 $[M + H]^+$ (anal. calcd. for $C_{23}H_{23}N_3O_4S$: m/z = 437.1).

*3-Methyl-8-(3-(methylsulfonyl)phenyl)-1-(tetrahydro-2H-pyran-4-yl)-1,3-dihydro-2H-imidazo[4,5-c]quinolin-2-one (**15**).* Synthesized from **4** (0.100 g, 0.28 mmol) and (3-(methylsulfonyl)phenyl)-boronic acid (0.082 g, 0.41 mmol) according to Method A to give **15** as a yellow solid (0.080 g, 72% yield); ^{1}H NMR (300 MHz, DMSO-d_6) δ 8.92 (s, 1H), 8.56 (s, 1H), 8.38 (s, 1H), 8.28−8.13 (m, 2H), 8.10−7.95 (m, 2H), 7.84 (m, 1H), 5.21−5.15 (m, 1H), 4.10−4.04 (m, 2H), 3.67−3.54 (m, 2H), 3.51 (s, 3H), 3.35 (s, 3H), 2.79−2.65 (m, 2H), 2.02−1.88 (m, 2H). ^{13}C NMR (101 MHz, DMSO-d_6) δ: 153.36, 144.75, 142.43, 141.24, 136.33, 134.29, 132.50, 132.04, 130.85, 128.71, 126.60, 126.04, 125.80, 123.84, 120.35, 115.65, 67.14 (2C), 43.96, 30.25 (2C), 27.71 (2C). LC-MS: t_R = 0.751 min (Purity = 97%); m/z = 438.1 $[M + H]^+$ (anal. calcd. for $C_{23}H_{23}N_3O_4S$: m/z = 437.1).

*3-Methyl-8-(5-(methylsulfonyl)pyridin-3-yl)-1-(tetrahydro-2H-pyran-4-yl)-1,3-dihydro-2H-imidazo[4,5-c]quinolin-2-one (**16**).* Synthesized from **4** (0.100 g, 0.28 mmol) and (5-(methylsulfonyl)pyridin-3-yl)boronic acid (0.041 g; 0.21 mmol) according to Method A to give **16** as a white solid (0.04 g, 66%); ^{1}H NMR (300 MHz, DMSO-d_6) δ 9.45 (s, 1H), 9.14 (d, J = 10.1 Hz, 1H), 8.97 (s, 1H), 8.82 (s, 1H), 8.75 (s, 1H), 8.63 (s, 1H), 8.19 (d, J = 10.5 Hz, 1H), 5.21−5.15 (m, 1H), 4.07−4.03 (m, 2H), 3.62−3.53 (m, 5H), 3.46 (s, 3H), 2.79−2.67 (m, 2H), 1.97−1.93 (m, 2H). ^{13}C NMR (151 MHz, DMSO-d_6) δ 153.32, 152.81, 147.99, 146.92, 144.84, 137.87, 136.05, 134.55, 134.52, 133.94, 133.30, 132.12, 128.72, 125.73, 123.88, 67.03, 66.80, 44.08 (2C), 30.14 (2C), 27.69. LC-MS: t_R = 0.657 min (Purity = 97%); m/z = 439.1 $[M + H]^+$ (anal. calcd. for $C_{22}H_{22}N_4O_4S$: m/z = 438.1).

*3-Methyl-8-(3-(methylsulfinyl)phenyl)-1-(tetrahydro-2H-pyran-4-yl)-1,3-dihydro-2H-imidazo[4,5-c]quinolin-2-one (**17**).* Synthesized from **4** (0.100 g, 0.28 mmol) and (3-(methylsulfinyl)phenyl)-boronic acid (0.076 g, 0.41 mmol) according to Method A to give **17** as a yellow solid (0.081 g, 70% yield); ^{1}H NMR (300 MHz, DMSO-d_6) δ 8.90 (s, 1H), 8.54 (s, 1H), 8.17−8.14 (m, 2H), 8.07−7.97 (m, 2H), 7.72−7.77 (m, 2H), 5.19−5.11 (m, 1H), 4.11−4.04 (m, 2H), 3.71−3.45 (m, 5H), 2.86 (s, 3H), 2.86−2.67 (m, 2H), 1.95−1.91 (m, 2H). ^{13}C NMR (101 MHz, DMSO-d_6) δ: 153.35, 148.14, 144.67, 141.07, 136.99, 134.10, 131.93, 130.59, 129.68, 128.66, 125.85, 123.77, 123.45, 122.47, 119.97, 115.65, 67.18 (2C), 43.78, 30.26 (2C), 27.69 (2C). LC-MS: t_R = 0.706 min (Purity = 96%); m/z = 422.1 $[M + H]^+$ (anal. calcd. for $C_{23}H_{23}N_3O_3S$: m/z = 421.1).

*3-Methyl-8-(2-methylpyridin-3-yl)-1-(tetrahydro-2H-pyran-4-yl)-1,3-dihydro-2H-imidazo[4,5-c]quinolin-2-one (**18**).* Synthesized from **4** (0.100 g, 0.28 mmol) and 2-methylpyridine-3-boronic acid (0.057 g, 0.41 mmol) according to Method A to give **18** as a white solid (0.056 g, 54% yield); ^{1}H NMR (600 MHz, DMSO-d_6) δ 8.93 (s, 1H), 8.54 (dd, J = 4.8, 1.8 Hz, 1H), 8.28 (d, J = 1.9 Hz, 1H), 8.15 (d, J = 8.7 Hz, 1H), 7.82 (dd, J = 7.7, 1.8 Hz, 1H), 7.70 (dd, J = 8.7, 1.8 Hz, 1H), 7.39 (dd, J = 7.6, 4.8 Hz, 1H), 5.04 (tt, J = 11.9, 4.4 Hz, 1H), 4.01 (dd, J = 11.6, 4.7 Hz, 2H), 3.53 (s, 3H), 3.49 (td, J = 12.1, 2.0 Hz, 2H), 2.76−2.66 (m, 2H), 2.57 (s, 3H), 1.92−1.85 (m, 2H). ^{13}C NMR (151 MHz, DMSO-d_6) δ 154.92, 152.78, 147.89, 143.65, 137.17, 137.01, 135.63, 133.36, 130.61, 127.91, 127.55, 123.18, 121.36, 121.07, 114.75, 66.43 (2C), 52.80, 29.44 (2C), 26.99, 23.17. LC-MS: t_R = 0.450 min (Purity = 96%); m/z = 375.2 $[M + H]^+$ (anal. calcd. for $C_{22}H_{22}N_4O_2$: m/z = 374.2).

*3-Methyl-8-(4-methylpyridin-3-yl)-1-(tetrahydro-2H-pyran-4-yl)-1,3-dihydro-2H-imidazo[4,5-c]quinolin-2-one (**19**).* Synthesized from **4** (0.100 g, 0.28 mmol) and 4-methylpyridine-3-boronic acid (0.057 g, 0.41 mmol) according to Method A to give **19** as a white solid (0.027 g, 27% yield); ^{1}H NMR (600 MHz, DMSO-d_6) δ 8.95 (s, 1H), 8.60 (s, 1H), 8.50 (d, J = 5.0 Hz, 1H), 8.29 (d, J = 1.9 Hz, 1H), 8.16 (d, J = 8.7 Hz, 1H), 7.71 (dd, J = 8.7, 1.8 Hz, 1H), 7.42 (d, J = 5.0 Hz, 1H), 5.05 (m, 1H), 4.00 (m, 2H), 3.53 (s, 3H), 3.49 (m, 2H), 2.70 (m, 2H), 2.41 (s, 3H), 1.90−1.84 (m, 2H). ^{13}C NMR (151 MHz, DMSO-d_6) δ: 152.86, 149.72, 148.39, 144.17, 143.79, 136.57, 135.10, 133.61, 130.74, 127.99, 127.89, 125.53, 123.24, 121.47, 114.90, 66.53 (2C), 53.67, 29.53 (2C), 27.15, 19.54. LC-MS: t_R = 0.533 min (Purity = 100%); m/z = 375.2 $[M + H]^+$ (anal. calcd. for $C_{22}H_{22}N_4O_2$: m/z = 374.2).

*8-(6-Amino-2-methylpyridin-3-yl)-3-methyl-1-(tetrahydro-2H-pyran-4-yl)-1,3-dihydro-2H-imidazo[4,5-c]quinolin-2-one (**20**).* 8-(6-Fluoro-2-methylpyridin-3-yl)-3-methyl-1-(oxan-4-yl)imidazo[4,5-*c*]quinolin-2-one (0.127 g, 32 mmol) obtained from **4** (0.148 g, 0.40 mmol) and (6-fluoro-2-methylpyridin-3-yl)boronic acid (0.076 g, 0.49 mmol) according to Method A was heated (120 °C) with sodium carbonate (0.173 g, 1.63 mmol) and tert-Butylamine (2 mL, 19 mmol) in DMSO (1.5 mL) for 7 days. After cooling, the reaction was diluted with water (5 mL) to precipitate the crude product to give a 0.100 g beige solid (50% conversion to the desired product 8-[6-(tert-butylamino)-2-methylpyridin-3-yl]-3-methyl-1-(oxan-4-yl)imidazo-[4,5-*c*]quinolin-2-one). The crude product was refluxed in TFA (3 mL, 39 mmol) at 80 °C for 16 h. Purification was performed using silica gel flash chromatography eluting a gradient of ethyl acetate in petroleum ether to give **20** as a white solid (0.021 mg, 45% yield); ^{1}H NMR (300 MHz, DMSO-d_6) δ 8.88 (s, 1H), 8.16 (s, 1H), 8.07 (d, J = 8.7 Hz, 1H), 7.63 (d, J = 8.8 Hz, 1H), 7.47 (d, J = 8.4 Hz, 1H), 6.44 (d, J = 8.4 Hz, 1H), 6.08 (s, 2H), 5.13−4.93 (m, 1H), 4.10−3.96 (m, 2H), 3.56−3.42 (m, 5H), 2.79−2.58 (m, 2H), 2.39 (s, 3H), 1.91−1.78 (m, 2H). ^{13}C NMR (151 MHz, DMSO) δ: 158.47, 152.88, 143.30, 139.01, 138.24, 132.93, 130.43, 128.25, 127.78, 123.60, 123.11, 120.44, 114.93, 105.87, 66.67 (2C), 52.89, 29.59 (2C), 27.14, 22.98. LC-MS: t_R = 0.279 min (Purity = 100%); m/z = 390.2 $[M + H]^+$ (anal. calcd. for $C_{22}H_{23}N_5O_2$: m/z = 389.2).

*8-(6-Aminopyridin-3-yl)-3-methyl-1-(tetrahydro-2H-pyran-4-yl)-1,3-dihydro-2H-imidazo[4,5-c]quinolin-2-one (**21**).* Synthesized from **4** (0.250 g, 0.69 mmol) and 2-aminopyridine-5-boronic acid, pinacol ester (0.182 g, 0.83 mmol) according to Method A to give **21** as a beige solid (0.025 g, 9% yield); ^{1}H NMR (300 MHz, DMSO-d_6) δ 8.84 (s, 1H), 8.45 (s, 1H), 8.33 (s, 1H), 8.07 (d, J = 8.9 Hz, 1H), 7.89 (d, J = 8.8 Hz, 2H), 6.60 (d, J = 8.6 Hz, 1H), 6.24 (s, 2H), 5.11 (s, 1H), 4.14−4.02 (m, 2H), 3.64−3.54 (m, 2H), 3.50 (s, 3H), 2.80−2.62 (m, 2H), 1.91 (d, J = 12.3 Hz, 2H). ^{13}C NMR (101 MHz, DMSO-d_6) δ 159.52, 152.90, 146.40, 143.56, 135.88, 135.66, 132.76, 131.24, 127.81, 124.81, 123.33, 123.16, 116.53, 115.42, 108.18, 66.76 (2C), 52.76,

https://doi.org/10.1021/acs.jmedchem.5c01417
J. Med. Chem. 2025, 68, 17736−17751

29.83 (2C), 27.18. LC-MS: t_R = 0.524 min (Purity = 100%); m/z = 376.2 $[M + H]^+$ (anal. calcd. for $C_{21}H_{21}N_5O_2$: m/z = 375.2).

*N-(5-(3-Methyl-2-oxo-1-(tetrahydro-2H-pyran-4-yl)-2,3-dihydro-1H-imidazo[4,5-c]quinolin-8-yl)pyridin-2-yl)acetamide (**22**).* Synthesized from **4** (0.150 g, 0.41 mmol) and (6-acetamidopyridin-3-yl)boronic acid (0.089 g, 0.49 mmol) according to Method A to give **22** as a beige solid (0.052 g, 28% yield); ^{1}H NMR (300 MHz, DMSO-d_6) δ 10.70 (s, 1H), 8.90 (s, 1H), 8.83 (d, J = 2.0 Hz, 1H), 8.49 (s, 1H), 8.32−8.22 (m, 2H), 8.15 (d, J = 8.8 Hz, 1H), 8.01 (d, J = 8.8 Hz, 1H), 5.23−5.08 (m, 1H), 4.13−4.02 (m, 2H), 3.60 (t, J = 11.7 Hz, 2H), 3.52 (s, 3H), 2.72 (td, J = 12.7, 8.0 Hz, 2H), 2.14 (s, 3H), 1.98−1.88 (m, 2H). ^{13}C NMR (101 MHz, DMSO-d_6) δ: 169.42, 152.90, 151.73, 146.22, 143.99, 136.56, 134.45, 133.47, 131.47, 130.49, 128.07, 125.11, 123.30, 118.60, 115.28, 113.31, 66.68 (2C), 29.76 (2C), 27.24, 23.97. LC-MS: t_R = 0.743 min (Purity = 96%); m/z = 418.2 $[M + H]^+$ (anal. calcd. for $C_{23}H_{23}N_5O_3$: m/z = 417.2).

*8-(2-Aminopyridin-4-yl)-3-methyl-1-(tetrahydro-2H-pyran-4-yl)-1,3-dihydro-2H-imidazo[4,5-c]quinolin-2-one (**23**).* tert-Butyl (4-(3-methyl-2-oxo-1-(tetrahydro-2H-pyran-4-yl)-2,3-dihydro-1H-imidazo-[4,5-c]quinolin-8-yl)pyridin-2-yl)carbamate (0.209 g, 0.44 mmol) crude product was obtained from **4** (0.200 g, 0.55 mmol) and Boc-2-aminopyridine-4-boronic acid pinacol ester (0.212 g, 0.66 mmol) according to Method A. Following Method B, in DCM:TFA (5 mL) gave **23** as a beige solid (0.123 g, 59% yield); ^{1}H NMR (300 MHz, DMSO-d_6) δ 8.91 (s, 1H), 8.46 (s, 1H), 8.21−8.01 (m, 2H), 7.88 (d, J = 8.9 Hz, 1H), 6.95 (d, J = 5.3 Hz, 1H), 6.84 (s, 1H), 6.14 (s, 2H), 5.25−4.94 (m, 1H), 4.13−4.03 (m, 2H), 3.67−3.40 (m, 5H), 2.80−2.62 (m, 2H), 2.01−1.83 (m, 2H). 13C NMR (101 MHz, DMSO-d_6) δ: 160.62, 152.88, 148.73, 147.82, 144.51, 135.98, 133.75, 131.45, 128.28, 124.93, 123.27, 119.05, 115.11, 110.23, 105.52, 66.77 (2C), 53.16, 29.82 (2C), 27.22. LC-MS: t_R = 0.562 min (Purity = 100%); m/z = 376.2 $[M + H]^+$ (anal. calcd. for $C_{21}H_{21}N_5O_2$: m/z = 375.2).

*3-Methyl-8-(1H-pyrrolo[2,3-b]pyridin-4-yl)-1-(tetrahydro-2H-pyran-4-yl)-1,3-dihydro-2H-imidazo[4,5-c]quinolin-2-one (**24**).* Synthesized from **4** (0.150 g, 0.41 mmol) and 1H-pyrrolo[2,3-b]pyridine, 4-(4,4,5,5-tetramethyl-1,3,2-dioxaborolan-2-yl) (0.114 g, 0.47 mmol) according to Method A to give **24** as a yellow solid (0.133 g, 80% yield); ^{1}H NMR (300 MHz, DMSO-d_6) δ 11.96 (s, 1H), 8.93 (s, 1H), 8.68 (s, 1H), 8.37 (d, J = 4.9 Hz, 1H), 8.22 (d, J = 8.7 Hz, 1H), 8.02 (d, J = 8.8 Hz, 1H), 7.72−7.64 (m, 1H), 7.37 (d, J = 4.9 Hz, 1H), 6.86−6.79 (m, 1H), 5.18−4.97 (m, 1H), 4.01 (dd, J = 11.8, 4.3 Hz, 2H), 3.54−3.40 (m, 5H), 2.82−2.64 (m, 2H), 2.00−1.88 (m, 2H). ^{13}C NMR (151 MHz, DMSO- d_6) δ: 152.78, 149.29, 144.27, 143.05, 139.61, 135.89, 133.64, 131.41, 128.19, 127.10, 126.41, 123.19, 120.70, 117.28, 115.15, 114.56, 98.87, 66.78 (2C), 53.62, 29.67 (2C), 27.12. LC-MS: t_R = 0.647 min (Purity = 100%); m/z = 400.2 $[M + H]^+$ (anal. calcd. for $C_{23}H_{21}N_5O_2$: m/z = 399.2).

*3-Methyl-8-(3-(methylsulfonyl)phenyl)-1-(piperidin-4-yl)-1,3-dihydro-2H-imidazo[4,5-c]quinolin-2-one (**25**).* Following Method B, *tert*-butyl 4-(3-methyl-8-(3-(methylsulfonyl)phenyl)-2-oxo-2,3-dihydro-1H-imidazo[4,5-c]quinolin-1-yl)piperidine-1-carboxylate (0.05 g, 0.09 mmol) in DCM:TFA (15 mL) gave **25** as a white solid (0.038 g; 93% yield); ^{1}H NMR (300 MHz, DMSO-d_6) δ 9.08 (s, 1H), 9.02 (s, 1H), 8.56 (s, 1H), 8.43 (s, 1H), 8.35−8.23 (m, 2H), 8.18 (d, J = 7.7 Hz, 1H), 8.02 (d, J = 7.7 Hz, 1H), 7.85 (t, J = 7.8 Hz, 1H), 5.31−5.30 (m, 1H), 3.54 (s, 3H), 3.48−3.44 (m, 2H), 3.35 (s, 3H), 3.34−3.12 (m, 2H), 3.00−2.87 (m, 2H), 2.29−2.25 (m, 2H). ^{13}C NMR (101 MHz, DMSO-d_6) δ: 153.27, 142.25, 141.01, 136.90, 132.90 (3C), 130.72 (3C), 126.60 (3C), 123.87, 120.12, 115.48, 52.69, 43.97 (2C), 43.46 (2C), 127.86, 26.55. LC-MS: t_R = 0.506 min (Purity = 98%); m/z = 437.1 $[M + H]^+$ (anal. calcd. for $C_{23}H_{24}N_4O_3S$: m/z = 436.2).

*1-(3-Fluoropiperidin-4-yl)-3-methyl-8-(3-(methylsulfonyl)-phenyl)-1,3-dihydro-2H-imidazo[4,5-c]quinolin-2-one (**26**).* Following Method B, *tert*-butyl 3-fluoro-4-(3-methyl-8-(3-(methylsulfonyl)-phenyl)-2-oxo-2,3-dihydro-1H-imidazo[4,5-c]quinolin-1-yl)-piperidine-1-carboxylate (0.05 g, 0.09 mmol) in DCM:TFA (15 mL) gave a mixture of diasteroisomers **26** as a white solid (0.034 g; 83%); ^{1}H NMR (300 MHz, DMSO-d_6) δ 9.02 (s, 1H), 8.96−8.95 (m, 2H), 8.84 (s, 1H), 8.52 (m, 2H), 8.45−7.95 (m, 10H), 7.85 (m, 2H), 5.92−4.96 (m, 4H), 3.59−3.53 (m, 6H), 3.34 (s, 6H), 3.21−3.13 (m, 2H), 3.04−2.89 (m, 2H), 2.97−2.66 (m, 2H), 2.63−2.58 (m, 2H), 2.14−2.10 (m, 2H), 1.91−1.87 (m, 2H). ^{13}C NMR (151 MHz, DMSO-d_6) δ 153.75, 153.12, 144.77, 144.69, 142.35, 142.30, 141.33, 141.23, 136.28, 134.29, 134.26, 132.62, 132.56, 132.47, 131.94, 131.90, 130.79, 130.74, 129.30, 128.87, 126.54, 126.48, 126.09, 126.04, 125.94, 125.83, 125.78, 123.97, 123.76, 119.62, 115.80, 115.67, 89.70, 88.97, 88.52, 87.79, 60.32, 60.21, 50.18, 50.03, 45.02, 44.89, 43.97, 30.23, 27.78, 27.63. LC-MS: t_R = 0.508 and 0.556 min (Purity = 98%); m/z = 455.1 $[M + H]^+$ (anal. calcd. for $C_{23}H_{23}FN_4O_3S$: m/z = 454.1).

*3-Methyl-1-(3-methylpiperidin-4-yl)-8-(3-(methylsulfonyl)-phenyl)-1,3-dihydro-2H-imidazo[4,5-c]quinolin-2-one (**27**).* Following Method B, *tert*-butyl 3-methyl-4-(3-methyl-8-(3-(methylsulfonyl)-phenyl)-2-oxo-2,3-dihydro-1H-imidazo[4,5-c]quinolin-1-yl)-piperidine-1-carboxylate (0.05 g, 0.09 mmol) in DCM:TFA (15 mL) gave a mixture of diasteroisomers **27** as a white solid (0.037 g; 90% yield); ^{1}H NMR (300 MHz, DMSO-d_6) δ 9.00−8.99 (m, 2H), 8.96 (s, 1H), 8.66 (s, 1H), 8.58 (s, 1H), 8.43−8.18 (m, 7H), 8.14−7.97 (m, 4H), 7.88−7.81(m, 2H), 5.45−5.41 (m, 1H), 4.96−4.88 (m, 1H), 3.55 (s, 3H), 3.52 (s, 3H), 3.34−3.30 (m, 15H), 3.03−2.99 (m, 1H), 2.90−2.87 (m, 1H), 2.77−2.73 (m, 1H), 2.39−2.28 (m, 1H), 2.09−2.04 (m, 1H), 1.16 (d, J = 7.0 Hz, 3H), 0.84 (d, J = 6.4 Hz, 3H). ^{13}C NMR (151 MHz, DMSO-d_6) δ: 153.99, 153.07, 144.62, 144.56, 142.36, 142.31, 141.41, 141.24, 136.94, 136.69, 134.17, 134.04, 132.77, 132.74, 131.88, 131.82, 130.67 (2C), 129.37, 128.99, 126.52, 126.46 (2C), 126.33, 126.23, 126.11, 123.96, 123.91, 119.75, 119.58, 115.72, 115.66, 58.70, 55.27, 48.90, 48.12, 44.11, 44.07, 43.80, 43.51, 32.24, 30.61, 27.75, 27.71, 26.75, 22.24, 15.15, 12.10. LC-MS: t_R = 0.537 and 0.554 min (Purity = 98%);. m/z = 451.2 $[M + H]^+$ (anal. for $C_{24}H_{26}N_4O_3S$: m/z = 450.2)

*1-(Azetidin-3-yl)-3-methyl-8-(3-(methylsulfonyl)phenyl)-1,3-dihydro-2H-imidazo[4,5-c]quinolin-2-one (**28**).* Following Method B, *tert*-butyl 3-(3-methyl-8-(3-(methylsulfonyl)phenyl)-2-oxo-2,3-dihydro-1H-imidazo[4,5-c]quinolin-1-yl)azetidine-1-carboxylate (0.05 g; 0.10 mmol) in DCM:TFA (15 mL) gave **28** as a white solid (0.035 g; 87% yield); ^{1}H NMR (300 MHz, DMSO-d_6) δ 9.03 (m, 2H), 8.50 (s, 1H), 8.38−8.28 (m, 2H), 8.22 (d, J = 8.8 Hz, 1H), 8.13−7.98 (m, 2H), 7.86 (t, J = 7.7 Hz, 1H), 6.23−6.12 (m, 1H), 4.88−4.85 (m, 2H), 4.48−4.42 (m, 2H), 3.60 (s, 3H), 3.37 (s, 3H). ^{13}C NMR (151 MHz, DMSO-d_6) δ 153.81, 144.38, 142.37, 141.47, 136.98, 134.17, 133.05, 131.52, 130.59, 128.80, 126.75, 126.52, 126.18, 123.82, 119.62, 115.67, 50.85 (2C), 47.48, 44.01, 27.79. LC-MS: t_R = 0.452 min (Purity = 98%); m/z = 409.1 $[M + H]^+$ (anal. calcd. for $C_{21}H_{20}N_4O_3S$: m/z = 408.1).

*3-Methyl-8-(2-methylpyridin-3-yl)-1-phenyl-1,3-dihydro-2H-imidazo[4,5-c]quinolin-2-one (**29**).* Synthesized from **4b** (0.150 g, 0.42 mmol) and 2-methylpyridine-3-boronic acid pinacol ester (0.111 g, 0.51 mmol) according to Method A to give **29** as a white solid (0.116 g, 74% yield); ^{1}H NMR (300 MHz, DMSO-d_6) δ 9.05 (s, 1H), 8.42 (dd, J = 4.6, 1.8 Hz, 1H), 8.12 (d, J = 8.8 Hz, 1H), 7.67−7.56 (m, 6H), 7.48 (dd, J = 7.9, 1.8 Hz, 1H), 7.26 (dd, J = 7.8, 4.8 Hz, 1H), 6.99 (d, J = 2.0 Hz, 1H), 3.62 (s, 3H), 2.22 (s, 3H). ^{13}C NMR (101 MHz, DMSO-d_6) δ: 154.67, 153.10, 148.05, 143.55, 137.09, 136.49, 135.46, 135.21, 133.85, 130.44, 130.01 (2C), 129.68, 128.86 (2C), 128.64, 127.97, 123.26, 121.49, 120.28, 114.33, 27.71, 23.15. LC-MS: t_R = 0.610 min (Purity = 100%); m/z = 367.2 $[M + H]^+$ (anal. calcd. for $C_{23}H_{18}N_4O$: m/z = 366.1).

*8-(6-Aminopyridin-3-yl)-3-methyl-1-phenyl-1,3-dihydro-2H-imidazo[4,5-c]quinolin-2-one (**30**).* Synthesized from **4b** (0.150 g, 0.42 mmol) and 2-aminopyridine-5-boronic acid pinacol ester (0.111 g, 0.51 mmol) according to Method A to give **30** as a beige solid (0.007 g, 4% yield); ^{1}H NMR (300 MHz, DMSO-d_6) δ 8.95 (s, 1H), 8.03 (d, J = 8.9 Hz, 1H), 7.86 (d, J = 2.4 Hz, 1H), 7.80 (d, J = 8.9 Hz, 1H), 7.76−7.62 (m, 5H), 7.39 (dd, J = 8.7, 2.6 Hz, 1H), 7.04 (s, 1H), 6.44 (d, J = 8.6 Hz, 1H), 6.19 (s, 2H), 3.60 (s, 3H). ^{13}C NMR (101 MHz, DMSO-d_6) δ 159.39, 153.04, 145.71, 143.34, 135.57, 135.12, 134.91, 132.90, 130.71, 129.93 (2C), 129.67, 129.08 (2C), 128.33, 124.81, 123.09, 122.65, 114.96, 107.93, 27.67.LC-MS: t_R = 0.587 min (Purity = 100%); m/z = 368.1 $[M + H]^+$ (anal. calcd. for $C_{22}H_{17}N_5O$: m/z = 367.1).

DMPK. All protocols for *in vitro* DMPK studies and mouse PK studies are available in the supplementary document. Animal studies were conducted following guidelines and policies as stipulated in the

https://doi.org/10.1021/acs.jmedchem.5c01417
J. Med. Chem. 2025, 68, 17736−17751

University of Cape Town Research Ethics Code for Use of Animals in Research and Teaching, after review and approval of the experimental protocol by the UCT Senate Animal Ethics Committee (protocol FHS-AEC 013/032).

■ ASSOCIATED CONTENT

Supporting Information

The Supporting Information is available free of charge at https://pubs.acs.org/doi/10.1021/acs.jmedchem.5c01417.

Synthesis of intermediates; analytical spectra of compounds profiled *in vivo*; parasitology methods; *Pv*PI4K and human kinase assays; *in vitro* ADME assays, and mouse pharmacokinetic and *in vivo* efficacy studies (PDF)

In vitro data of all final compounds (mean IC_{50} values ± standard deviation (SD) or standard error (SE)) (CSV)

Molecular formula strings (CSV)

PfPI4K-AZD0156 (PDB)

PfPI4K-Compound 18 (PDB)

HsATM-Compound 18 (PDB)

■ AUTHOR INFORMATION

Corresponding Author

Kelly Chibale − *Holistic Drug Discovery and Development Centre (H3D), Department of Chemistry, University of Cape Town, Rondebosch 7701, South Africa; South African Medical Research Council Drug Discovery and Development Research Unit, Department of Chemistry and Institute of Infectious Disease and Molecular Medicine, University of Cape Town, Rondebosch 7701, South Africa;* orcid.org/0000-0002-1327-4727; Phone: +27216502553; Email: kelly.chibale@uct.ac.za

Authors

Godwin A. Dziwornu − *Holistic Drug Discovery and Development Centre (H3D), Department of Chemistry, University of Cape Town, Rondebosch 7701, South Africa;* orcid.org/0000-0003-1668-8818

Mmakwena M. Mmonwa − *Department of Chemistry, University of Cape Town, Rondebosch 7701, South Africa;* Present Address: Department of Chemistry, KwaDlangezwa Campus, University of Zululand, Empangeni 3886, South Africa

Dina Coertzen − *Department of Biochemistry, Genetics and Microbiology, Institute for Sustainable Malaria Control, University of Pretoria, Pretoria 0028, South Africa*

Liezl Krugmann − *Holistic Drug Discovery and Development Centre (H3D), Institute of Infectious Disease and Molecular Medicine, University of Cape Town, Cape Town 7925, South Africa*

Nicolaas Salomane − *Holistic Drug Discovery and Development Centre (H3D), Institute of Infectious Disease and Molecular Medicine, University of Cape Town, Cape Town 7925, South Africa*

Meta Leshabane − *Wellcome Sanger Institute, Hinxton CB10 1SA, U.K.*

Jean Thomas − *Department of Biochemistry, Genetics and Microbiology, Institute for Sustainable Malaria Control, University of Pretoria, Pretoria 0028, South Africa*

Shante da Rocha − *Department of Biochemistry, Genetics and Microbiology, Institute for Sustainable Malaria Control, University of Pretoria, Pretoria 0028, South Africa*

Janette Reader − *Department of Biochemistry, Genetics and Microbiology, Institute for Sustainable Malaria Control, University of Pretoria, Pretoria 0028, South Africa*

Keabetswe Masike − *Holistic Drug Discovery and Development Centre (H3D), Institute of Infectious Disease and Molecular Medicine, University of Cape Town, Cape Town 7925, South Africa*

Mathew Njoroge − *Holistic Drug Discovery and Development Centre (H3D), Institute of Infectious Disease and Molecular Medicine, University of Cape Town, Cape Town 7925, South Africa*

Nicole Sevilleno − *Wellcome Sanger Institute, Hinxton CB10 1SA, U.K.*

Rachael Coyle − *Wellcome Sanger Institute, Hinxton CB10 1SA, U.K.*

Nonlawat Boonyalai − *Biological Chemistry and Drug Discovery, Wellcome Centre for Anti-Infectives Research, University of Dundee, Dundee DD1 5EH, U.K.*

Emily Mayville − *Department of Microbiology and Immunology, Columbia University Medical Center, Hammer Health Sciences Center, New York, New York 10032, United States; Center for Malaria Therapeutics and Antimicrobial Resistance, Division of Infectious Diseases, Department of Medicine, Columbia University Irving Medical Center, New York, New York 10032, United States*

Marcus C. S. Lee − *Wellcome Sanger Institute, Hinxton CB10 1SA, U.K.; Biological Chemistry and Drug Discovery, Wellcome Centre for Anti-Infectives Research, University of Dundee, Dundee DD1 5EH, U.K.*

David A. Fidock − *Department of Microbiology and Immunology, Columbia University Medical Center, Hammer Health Sciences Center, New York, New York 10032, United States; Center for Malaria Therapeutics and Antimicrobial Resistance, Division of Infectious Diseases, Department of Medicine, Columbia University Irving Medical Center, New York, New York 10032, United States*

Lauren B. Coulson − *Holistic Drug Discovery and Development Centre (H3D), Institute of Infectious Disease and Molecular Medicine, University of Cape Town, Cape Town 7925, South Africa;* orcid.org/0000-0003-4699-0428

John G. Woodland − *Holistic Drug Discovery and Development Centre (H3D), Department of Chemistry, University of Cape Town, Rondebosch 7701, South Africa; South African Medical Research Council Drug Discovery and Development Research Unit, Department of Chemistry and Institute of Infectious Disease and Molecular Medicine, University of Cape Town, Rondebosch 7701, South Africa;* orcid.org/0000-0001-6273-5596

Kathryn J. Wicht − *Holistic Drug Discovery and Development Centre (H3D), Department of Chemistry, University of Cape Town, Rondebosch 7701, South Africa; South African Medical Research Council Drug Discovery and Development Research Unit, Department of Chemistry and Institute of Infectious Disease and Molecular Medicine, University of Cape Town, Rondebosch 7701, South Africa;* orcid.org/0000-0001-6145-9956

Sandeep R. Ghorpade − *Holistic Drug Discovery and Development Centre (H3D), Department of Chemistry, University of Cape Town, Rondebosch 7701, South Africa;* orcid.org/0000-0002-9311-1572

Lyn-Marié Birkholtz − *Department of Biochemistry, Genetics and Microbiology, Institute for Sustainable Malaria Control, University of Pretoria, Pretoria 0028, South Africa;*

Department of Biochemistry, Stellenbosch University, Stellenbosch 7601, South Africa; orcid.org/0000-0001-5888-2905

Complete contact information is available at: https://pubs.acs.org/10.1021/acs.jmedchem.5c01417

Author Contributions

⋈GAD and MMM contributed equally to this work. GAD and MMM designed and synthesized the compounds and composed the manuscript. DC, ML, JT, SdR, and JR conducted the transmission-blocking assays. NSal conducted the *Pv*PI4K enzyme assays. KM conducted and analyzed the logD and solubility assays. MN analyzed the *in vitro* DMPK assays and contributed to *in vivo* PK analysis and human PK predictions. LG conducted and interpreted the *in vivo* PK studies and NSG study and wrote the *in vivo* PK studies, and NSG study sections. NSev, NB, and RC performed the *Pf*PI4K mutant cross-resistance assays. MCSL planned the *Pf*PI4K mutant cross-resistance experiments and supervised the study. LBC supervised and analyzed the *Pv*PI4K enzyme assays. EM conducted the MIR study, with supervision from DAF. JW, KJW, and SRG provided scientific guidance. DC and LMB supervised the transmission-blocking assays, analyzed and interpreted the data. KC conceived the project and provided scientific guidance. LMB, DAF, and KC were responsible for funding acquisition. All authors edited the manuscript and have given approval to the final version of the manuscript.

Funding

The University of Cape Town, South African Medical Research Council (SAMRC), and South African Research Chairs Initiative (SARChI) of the Department of Science and Innovation (DSI), administered through the South African National Research Foundation (NRF), are gratefully acknowledged for support (KC). KC is the Neville Isdell Chair in African-centric Drug Discovery and Development and thanks Neville Isdell for generously funding the chair. The transmission-blocking assay platform was supported by grants from the Medicines for Malaria Venture (LMB: RD-19−001), the SAMRC, and the DSI SARChI Grants managed by the NRF (LMB UID: 84627). The *Plasmodium* AReBar assay platform was supported by Medicines for Malaria Venture (MCSL: RD-18−0005). The *Plasmodium* kinase platform was supported by the Future Leaders−African Independent Research (FLAIR) Fellowship Programme, a partnership between the African Academy of Sciences and the Royal Society funded by the UK Government's Global Challenges Research (to LBC). The *in vivo* studies were supported by the Global Health Grants (Number OPP1066878) received from the Bill and Melinda Gates Foundation (BMGF), the Division of Intramural Research of the NIAID/NIH. DF gratefully acknowledges funding support from the Medicines for Malaria Venture (MMV; 08/0015) and the NIH (R01 AI185559).

Notes

The authors declare no competing financial interest.

■ ACKNOWLEDGMENTS

The authors acknowledge Dr. Stephen Fienberg, H3D, University of Cape Town, for performing the docking studies of the reported compounds against *Pf*PI4K and *Hs*PI4K*β* and generating all the associated docking images. Dr. James Duffy and Elodie Chenu from Medicines for Malaria Venture (MMV) are thanked for scientific discussions throughout the course of the study. MMV is thanked for providing access to a few different parasitology assay platforms.

■ ABBREVIATIONS USED

ABS, asexual blood stage; ADME, absorption, distribution, metabolism, and excretion; ATM, ataxia-telangiectasia-mutated; ATP, adenosine triphosphate; ATR, ataxia telangiectasia and Rad3-related; AUC, area under the curve; DCM, dichloromethane; DIPEA, diisopropylethylamine; DMA, dimethylacetamide; DMF, *N*,*N*-dimethylformamide; DMF-DMA, *N*,*N*-dimethylformamide dimethyl acetal; DMPK, drug metabolism and pharmacokinetics; DPPA, diphenylphosphoryl azide; ED_{90}, the effective dose for 90% reduction in parasitaemia; HATU, 1-[Bis(dimethylamino)methylene]-1*H*-1,2,3-triazolo[4,5-*b*]-pyridinium 3-oxid hexafluorophosphate; iGC, immature gametocytes; K_2CO_3, potassium carbonate; LCMS, liquid chromatography−mass spectrometry; lGC, late-stage gametocytes; LiOH, lithium hydroxide; MAP4K4, mitogen-activated protein kinase kinase kinase kinase 4; MeOH, methanol; MINK1, misshapen-like kinase 1; mTOR, mammalian target of rapamycin; NaH, sodium hydride; NaOH, sodium hydroxide; NEt_3, triethylamine; NMR, nuclear magnetic resonance; PCy_3, tricyclohexylphosphine; $PdCl_2(PPh_3)_2$, bis-(triphenylphosphine)palladium(II) chloride; PI4K, phosphatidylinositol-4-kinase III*β*; SAR, structure−activity relationship; SMILES, simplified molecular input line entry system; TFA, trifluoroacetic acid; THF, tetrahydrofuran; THP, tetrahydropyran; tPSA, topological polar surface area

■ REFERENCES

(1) Blasco, B.; Leroy, D.; Fidock, D. A. Antimalarial Drug Resistance: Linking Plasmodium Falciparum Parasite Biology to the Clinic. *Nat. Med.* **2017**, *23* (8), 917−928.

(2) Madhav, H.; Hoda, N. An Insight into the Recent Development of the Clinical Candidates for the Treatment of Malaria and Their Target Proteins. *Eur. J. Med. Chem.* **2021**, *210*, No. 112955.

(3) World Health Organization. *World Malaria Report* 2023.

(4) Rosenthal, P. J.; Asua, V.; Bailey, J. A.; Conrad, M. D.; Ishengoma, D. S.; Kamya, M. R.; Rasmussen, C.; Tadesse, F. G.; Uwimana, A.; Fidock, D. A. The Emergence of Artemisinin Partial Resistance in Africa: How Do We Respond? *Lancet Infect. Dis.* **2024**, *24* (9), e591−e600.

(5) Björkman, A.; Gil, P.; Alifrangis, M. Alarming Plasmodium Falciparum Resistance to Artemisinin-Based Combination Therapy in Africa: The Critical Role of the Partner Drug. *Lancet Infect. Dis.* **2024**, *24* (9), e540−e541.

(6) White, N. J.; Chotivanich, K. Artemisinin-Resistant Malaria. *Clin. Microbiol. Rev.* **2024**, *37* (4), No. e00109-24, DOI: 10.1128/cmr.00109-24.

(7) Laurens, M. B. RTS,S/AS01 Vaccine (Mosquirix): An Overview. *Hum. Vaccines Immunother.* **2020**, *16* (3), 480−489.

(8) Datoo, M. S.; Dicko, A.; Tinto, H.; Ouédraogo, J.-B.; Hamaluba, M.; Olotu, A.; Beaumont, E.; Lopez, F. R.; Natama, H. M.; Weston, S.; Chemba, M.; Compaore, Y. D.; Issiaka, D.; Salou, D.; Some, A. M.; Omenda, S.; Lawrie, A.; Bejon, P.; Rao, H.; Chandramohan, D.; Roberts, R.; Bharati, S.; Stockdale, L.; Gairola, S.; Greenwood, B. M.; Ewer, K. J.; Bradley, J.; Kulkarni, P. S.; Shaligram, U.; Hill, A. V. S.; Mahamar, A.; Sanogo, K.; Sidibe, Y.; Diarra, K.; Samassekou, M.; Attaher, O.; Tapily, A.; Diallo, M.; Dicko, O. M.; Kaya, M.; Maguiraga, S. O.; Sankare, Y.; Yalcouye, H.; Diarra, S.; Niambele, S. M.; Thera, I.; Sagara, I.; Sylla, M.; Dolo, A.; Misidai, N.; Simando, S.; Msami, H.; Juma, O.; Gutapaka, N.; Paul, R.; Mswata, S.; Sasamalo, I.; Johaness, K.; Sultan, M.; Alexander, A.; Kimaro, I.; Lwanga, K.; Mtungwe, M.; Khamis, K.; Rugarabam, L.; Kalinga, W.; Mohammed, M.; Kamange, J.; Msangi, J.; Mwaijande, B.; Mtaka, I.; Mhapa, M.; Mlaganile, T.; Mbaga, T.; Yerbanga, R. S.; Samtouma, W.; Sienou, A. A.; Kabre, Z.;

Ouedraogo, W. J. M.; Yarbanga, G. A. B.; Zongo, I.; Savadogo, H.; Sanon, J.; Compaore, J.; Kere, I.; Yoni, F. L.; Sanre, T. M.; Ouattara, S. B.; Provstgaard-Morys, S.; Woods, D.; Snow, R. W.; Amek, N.; Ngetsa, C. J.; Ochola-Oyier, L. I.; Musyoki, J.; Munene, M.; Mumba, N.; Adetifa, U. J.; Muiruri, C. M.; Mwawaka, J. S.; Mwaganyuma, M. H.; Ndichu, M. N.; Weya, J. O.; Njogu, K.; Grant, J.; Webster, J.; Lakhkar, A.; Ido, N. F. A.; Traore, O.; Tahita, M. C.; Bonko, M. dit A.; Rouamba, T.; Ouedraogo, D. F.; Soma, R.; Millogo, A.; Ouedraogo, E.; Sorgho, F.; Konate, F.; Valea, I. Safety and Efficacy of Malaria Vaccine Candidate R21/Matrix-M in African Children: A Multicentre, Double-Blind, Randomised, Phase 3 Trial. *Lancet* **2024**, *403* (10426), 533−544.

(9) Cairns, M.; Ceesay, S. J.; Sagara, I.; Zongo, I.; Kessely, H.; Gamougam, K.; Diallo, A.; Ogboi, J. S.; Moroso, D.; Van Hulle, S.; Eloike, T.; Snell, P.; Scott, S.; Merle, C.; Bojang, K.; Ouedraogo, J. B.; Dicko, A.; Ndiaye, J.-L.; Milligan, P. Effectiveness of Seasonal Malaria Chemoprevention (SMC) Treatments When SMC Is Implemented at Scale: Case−Control Studies in 5 Countries. *PLoS Med.* **2021**, *18* (9), No. e1003727.

(10) El Gaaloul, M.; Tchouatieu, A. M.; Kayentao, K.; Campo, B.; Buffet, B.; Ramachandruni, H.; Ndiaye, J. L.; Wells, T. N. C.; Audibert, C.; Achan, J.; Donini, C.; Barsosio, H. C.; Tinto, H. Chemoprevention of Malaria with Long-Acting Oral and Injectable Drugs: An Updated Target Product Profile. *Malar. J.* **2024**, *23* (1), No. 315.

(11) Njoroge, M.; Njuguna, N. M.; Mutai, P.; Ongarora, D. S. B.; Smith, P. W.; Chibale, K. Recent Approaches to Chemical Discovery and Development Against Malaria and the Neglected Tropical Diseases Human African Trypanosomiasis and Schistosomiasis. *Chem. Rev.* **2014**, *114* (22), 11138−11163.

(12) Nzila, A.; Ma, Z.; Chibale, K. Drug Repositioning in the Treatment of Malaria and TB. *Future Med. Chem.* **2011**, *3* (11), 1413−1426.

(13) Woodland, J. G.; Coertzen, D.; Wicht, K. J.; Hidalgo, V. F.; Pasaje, C. F. A.; Godoy, L. C.; Qahash, T.; Mmonwa, M. M.; Dziwornu, G. A.; Wambua, L.; Harries, S.; Korkor, C. M.; Njoroge, M.; Gibhard, L.; Taylor, D.; Leshabane, M.; Langeveld, H.; Rabie, T.; Reader, J.; van der Watt, M.; Venter, N.; Erlank, E.; Aswat, A. S.; Koekemoer, L. L.; Yeo, T.; Jeon, J. H.; Fidock, D. A.; Gamo, F. J.; Wittlin, S.; Niles, J. C.; Llinas, M.; Coulson, L. B.; Birkholtz, L.-M.; Chibale, K. The ATM Kinase Inhibitor AZD0156 Is a Potent Inhibitor of Plasmodium Phosphatidylinositol 4-Kinase (PI4Kβ) and Is an Attractive Candidate for Medicinal Chemistry Optimisation. *Angew. Chem., Int. Ed.* **2025**, No. e202425206.

(14) Paquet, T.; Le Manach, C.; Cabrera, D. G.; Younis, Y.; Henrich, P. P.; Abraham, T. S.; Lee, M. C. S.; Basak, R.; Ghidelli-Disse, S.; Lafuente-Monasterio, M. J.; Bantscheff, M.; Ruecker, A.; Blagborough, A. M.; Zakutansky, S. E.; Zeeman, A.-M.; White, K. L.; Shackleford, D. M.; Mannila, J.; Morizzi, J.; Scheurer, C.; Angulo-Barturen, I.; Martínez, M. S.; Ferrer, S.; Sanz, L. M.; Gamo, F. J.; Reader, J.; Botha, M.; Dechering, K. J.; Sauerwein, R. W.; Tungtaeng, A.; Vanachayangkul, P.; Lim, C. S.; Burrows, J.; Witty, M. J.; Marsh, K. C.; Bodenreider, C.; Rochford, R.; Solapure, S. M.; Jiménez-Díaz, M. B.; Wittlin, S.; Charman, S. A.; Donini, C.; Campo, B.; Birkholtz, L.-M.; Hanson, K. K.; Drewes, G.; Kocken, C. H. M.; Delves, M. J.; Leroy, D.; Fidock, D. A.; Waterson, D.; Street, L. J.; Chibale, K. Antimalarial Efficacy of MMV390048, an Inhibitor of *Plasmodium* Phosphatidylinositol 4-Kinase. *Sci. Transl. Med.* **2017**, *9* (387), No. eaad9735.

(15) Brunschwig, C.; Lawrence, N.; Taylor, D.; Abay, E.; Njoroge, M.; Basarab, G. S.; Le Manach, C.; Paquet, T.; Cabrera, D. G.; Nchinda, A. T.; de Kock, C.; Wiesner, L.; Denti, P.; Waterson, D.; Blasco, B.; Leroy, D.; Witty, M. J.; Donini, C.; Duffy, J.; Wittlin, S.; White, K. L.; Charman, S. A.; Jiménez-Díaz, M. B.; Angulo-Barturen, I.; Herreros, E.; Gamo, F. J.; Rochford, R.; Mancama, D.; Coetzer, T. L.; van der Watt, M. E.; Reader, J.; Birkholtz, L.-M.; Marsh, K. C.; Solapure, S. M.; Burke, J. E.; McPhail, J. A.; Vanaerschot, M.; Fidock, D. A.; Fish, P. V.; Siegl, P.; Smith, D. A.; Wirjanata, G.; Noviyanti, R.; Price, R. N.; Marfurt, J.; Silue, K. D.; Street, L. J.; Chibale, K. UCT943, a Next-Generation Plasmodium Falciparum PI4K Inhibitor Preclinical Candidate for the Treatment of Malaria. *Antimicrob. Agents Chemother.* **2018**, *62* (9), No. 10-1128.

(16) McNamara, C. W.; Lee, M. C. S.; Lim, C. S.; Lim, S. H.; Roland, J.; Nagle, A.; Simon, O.; Yeung, B. K. S.; Chatterjee, A. K.; McCormack, S. L.; Manary, M. J.; Zeeman, A.-M.; Dechering, K. J.; Kumar, T. R. S.; Henrich, P. P.; Gagaring, K.; Ibanez, M.; Kato, N.; Kuhen, K. L.; Fischli, C.; Rottmann, M.; Plouffe, D. M.; Bursulaya, B.; Meister, S.; Rameh, L.; Trappe, J.; Haasen, D.; Timmerman, M.; Sauerwein, R. W.; Suwanarusk, R.; Russell, B.; Renia, L.; Nosten, F.; Tully, D. C.; Kocken, C. H. M.; Glynne, R. J.; Bodenreider, C.; Fidock, D. A.; Diagana, T. T.; Winzeler, E. A. Targeting Plasmodium PI(4)K to Eliminate Malaria. *Nature* **2013**, *504* (7479), 248−253.

(17) Pike, K. G.; Barlaam, B.; Cadogan, E.; Campbell, A.; Chen, Y.; Colclough, N.; Davies, N. L.; de-Almeida, C.; Degorce, S. L.; Didelot, M.; Dishington, A.; Ducray, R.; Durant, S. T.; Hassall, L. A.; Holmes, J.; Hughes, G. D.; MacFaul, P. A.; Mulholland, K. R.; McGuire, T. M.; Ouvry, G.; Pass, M.; Robb, G.; Stratton, N.; Wang, Z.; Wilson, J.; Zhai, B.; Zhao, K.; Al-Huniti, N. The Identification of Potent, Selective, and Orally Available Inhibitors of Ataxia Telangiectasia Mutated (ATM) Kinase: The Discovery of AZD0156 (8-{6-[3-(Dimethylamino)-Propoxy]Pyridin-3-Yl}-3-Methyl-1-(Tetrahydro-2 *H* -Pyran-4-Yl)-1,3-Dihydro-2 *H* -Imidazo[4,5- *c*]Quinolin-2-One). *J. Med. Chem.* **2018**, *61* (9), 3823−3841.

(18) Fienberg, S.; Eyermann, C. J.; Arendse, L. B.; Basarab, G. S.; McPhail, J. A.; Burke, J. E.; Chibale, K. Structural Basis for Inhibitor Potency and Selectivity of *Plasmodium Falciparum* Phosphatidylinositol 4-Kinase Inhibitors. *ACS Infect. Dis.* **2020**, *6* (11), 3048−3063.

(19) Arendse, L. B.; Murithi, J. M.; Qahash, T.; Pasaje, C. F. A.; Godoy, L. C.; Dey, S.; Gibhard, L.; Ghidelli-Disse, S.; Drewes, G.; Bantscheff, M.; Lafuente-Monasterio, M. J.; Fienberg, S.; Wambua, L.; Gachuhi, S.; Coertzen, D.; van der Watt, M.; Reader, J.; Aswat, A. S.; Erlank, E.; Venter, N.; Mittal, N.; Luth, M. R.; Ottilie, S.; Winzeler, E. A.; Koekemoer, L. L.; Birkholtz, L.-M.; Niles, J. C.; Llinás, M.; Fidock, D. A.; Chibale, K. The Anticancer Human MTOR Inhibitor Sapanisertib Potently Inhibits Multiple *Plasmodium* Kinases and Life Cycle Stages. *Sci. Transl. Med.* **2022**, *14* (667), No. eabo7219.

(20) Naude, M.; van Heerden, A.; Reader, J.; van der Watt, M.; Niemand, J.; Joubert, D.; Siciliano, G.; Alano, P.; Njoroge, M.; Chibale, K.; Herreros, E.; Leroy, D.; Birkholtz, L.-M. Eliminating Malaria Transmission Requires Targeting Immature and Mature Gametocytes through Lipoidal Uptake of Antimalarials. *Nat. Commun.* **2024**, *15* (1), No. 9896.

(21) Flannery, E. L.; Kangwanrangsan, N.; Chuenchob, V.; Roobsoong, W.; Fishbaugher, M.; Zhou, K.; Billman, Z. P.; Martinson, T.; Olsen, T. M.; Schäfer, C.; Campo, B.; Murphy, S. C.; Mikolajczak, S. A.; Kappe, S. H. I.; Sattabongkot, J. Plasmodium Vivax Latent Liver Infection Is Characterized by Persistent Hypnozoites, Hypnozoite-Derived Schizonts, and Time-Dependent Efficacy of Primaquine. *Mol. Ther. Methods Clin. Dev.* **2022**, *26*, 427−440.

(22) Ruecker, A.; Mathias, D. K.; Straschil, U.; Churcher, T. S.; Dinglasan, R. R.; Leroy, D.; Sinden, R. E.; Delves, M. J. A Male and Female Gametocyte Functional Viability Assay To Identify Biologically Relevant Malaria Transmission-Blocking Drugs. *Antimicrob. Agents Chemother.* **2014**, *58* (12), 7292−7302.

(23) Baragaña, B.; Hallyburton, I.; Lee, M. C. S.; Norcross, N. R.; Grimaldi, R.; Otto, T. D.; Proto, W. R.; Blagborough, A. M.; Meister, S.; Wirjanata, G.; Ruecker, A.; Upton, L. M.; Abraham, T. S.; Almeida, M. J.; Pradhan, A.; Porzelle, A.; Martínez, M. S.; Bolscher, J. M.; Woodland, A.; Luksch, T.; Norval, S.; Zuccotto, F.; Thomas, J.; Simeons, F.; Stojanovski, L.; Osuna-Cabello, M.; Brock, P. M.; Churcher, T. S.; Sala, K. A.; Zakutansky, S. E.; Jiménez-Díaz, M. B.; Sanz, L. M.; Riley, J.; Basak, R.; Campbell, M.; Avery, V. M.; Sauerwein, R. W.; Dechering, K. J.; Noviyanti, R.; Campo, B.; Frearson, J. A.; Angulo-Barturen, I.; Ferrer-Bazaga, S.; Gamo, F. J.; Wyatt, P. G.; Leroy, D.; Siegl, P.; Delves, M. J.; Kyle, D. E.; Wittlin, S.; Marfurt, J.; Price, R. N.; Sinden, R. E.; Winzeler, E. A.; Charman, S. A.; Bebrevska, L.; Gray, D. W.; Campbell, S.; Fairlamb, A. H.; Willis, P. A.; Rayner, J. C.; Fidock, D. A.; Read, K. D.; Gilbert, I. H. A Novel Multiple-Stage Antimalarial Agent That Inhibits Protein Synthesis. *Nature* **2015**, *522* (7556), 315−320.

(24) Qiu, D.; Pei, J. V.; Rosling, J. E. O.; Thathy, V.; Li, D.; Xue, Y.; Tanner, J. D.; Penington, J. S.; Aw, Y. T. V.; Aw, J. Y. H.; Xu, G.;

https://doi.org/10.1021/acs.jmedchem.5c01417
J. Med. Chem. 2025, 68, 17736−17751

Tripathi, A. K.; Gnadig, N. F.; Yeo, T.; Fairhurst, K. J.; Stokes, B. H.; Murithi, J. M.; Kümpornsin, K.; Hasemer, H.; Dennis, A. S. M.; Ridgway, M. C.; Schmitt, E. K.; Straimer, J.; Papenfuss, A. T.; Lee, M. C. S.; Corry, B.; Sinnis, P.; Fidock, D. A.; van Dooren, G. G.; Kirk, K.; Lehane, A. M. A G358S Mutation in the Plasmodium Falciparum Na+ Pump PfATP4 Confers Clinically-Relevant Resistance to Cipargamin. *Nat. Commun.* **2022**, *13* (1), No. 5746.

(25) LaMonte, G.; Lim, M. Y.-X.; Wree, M.; Reimer, C.; Nachon, M.; Corey, V.; Gedeck, P.; Plouffe, D.; Du, A.; Figueroa, N.; Yeung, B.; Bifani, P.; Winzeler, E. A. Mutations in the Plasmodium Falciparum Cyclic Amine Resistance Locus (PfCARL) Confer Multidrug Resistance. *mBio* **2016**, *7* (4), No. e01018-16.

(26) Stickles, A. M.; de Almeida, M. J.; Morrisey, J. M.; Sheridan, K. A.; Forquer, I. P.; Nilsen, A.; Winter, R. W.; Burrows, J. N.; Fidock, D. A.; Vaidya, A. B.; Riscoe, M. K. Subtle Changes in Endochin-Like Quinolone Structure Alter the Site of Inhibition within the Cytochrome Bc_1 Complex of Plasmodium Falciparum. *Antimicrob. Agents Chemother.* **2015**, *59* (4), 1977−1982.

(27) Carrasquilla, M.; Drammeh, N. F.; Rawat, M.; Sanderson, T.; Zenonos, Z.; Rayner, J. C.; Lee, M. C. S. Barcoding Genetically Distinct Plasmodium Falciparum Strains for Comparative Assessment of Fitness and Antimalarial Drug Resistance. *mBio* **2022**, *13* (5), No. e00937-22, DOI: 10.1128/mbio.00937-22.

(28) Kato, N.; Comer, E.; Sakata-Kato, T.; Sharma, A.; Sharma, M.; Maetani, M.; Bastien, J.; Brancucci, N. M.; Bittker, J. A.; Corey, V.; Clarke, D.; Derbyshire, E. R.; Dornan, G. L.; Duffy, S.; Eckley, S.; Itoe, M. A.; Koolen, K. M. J.; Lewis, T. A.; Lui, P. S.; Lukens, A. K.; Lund, E.; March, S.; Meibalan, E.; Meier, B. C.; McPhail, J. A.; Mitasev, B.; Moss, E. L.; Sayes, M.; Van Gessel, Y.; Wawer, M. J.; Yoshinaga, T.; Zeeman, A.-M.; Avery, V. M.; Bhatia, S. N.; Burke, J. E.; Catteruccia, F.; Clardy, J. C.; Clemons, P. A.; Dechering, K. J.; Duvall, J. R.; Foley, M. A.; Gusovsky, F.; Kocken, C. H. M.; Marti, M.; Morningstar, M. L.; Munoz, B.; Neafsey, D. E.; Sharma, A.; Winzeler, E. A.; Wirth, D. F.; Scherer, C. A.; Schreiber, S. L. Diversity-Oriented Synthesis Yields Novel Multistage Antimalarial Inhibitors. *Nature* **2016**, *538* (7625), 344−349.

(29) Arendse, L. B.; Wyllie, S.; Chibale, K.; Gilbert, I. H. *Plasmodium* Kinases as Potential Drug Targets for Malaria: Challenges and Opportunities. *ACS Infect. Dis.* **2021**, *7* (3), 518−534.

(30) Yang, T.; Ottilie, S.; Istvan, E. S.; Godinez-Macias, K. P.; Lukens, A. K.; Baragaña, B.; Campo, B.; Walpole, C.; Niles, J. C.; Chibale, K.; Dechering, K. J.; Llinás, M.; Lee, M. C. S.; Kato, N.; Wyllie, S.; McNamara, C. W.; Gamo, F. J.; Burrows, J.; Fidock, D. A.; Goldberg, D. E.; Gilbert, I. H.; Wirth, D. F.; Winzeler, E. A. MalDA, Accelerating Malaria Drug Discovery. *Trends Parasitol.* **2021**, *37* (6), 493−507.

(31) Coulson, L. B.; Chibale, K. Multi-target Antimalarials as a Strategy to Reduce Resistance Risk. In *Polypharmacology*; Wiley, 2025; pp 423−436.

(32) Lempiäinen, H.; Halazonetis, T. D. Emerging Common Themes in Regulation of PIKKs and PI3Ks. *EMBO J.* **2009**, *28* (20), 3067−3073.

(33) Degorce, S. L.; Barlaam, B.; Cadogan, E.; Dishington, A.; Ducray, R.; Glossop, S. C.; Hassall, L. A.; Lach, F.; Lau, A.; McGuire, T. M.; Nowak, T.; Ouvry, G.; Pike, K. G.; Thomason, A. G. Discovery of Novel 3-Quinoline Carboxamides as Potent, Selective, and Orally Bioavailable Inhibitors of Ataxia Telangiectasia Mutated (ATM) Kinase. *J. Med. Chem.* **2016**, *59* (13), 6281−6292.

(34) Stakyte, K.; Rotheneder, M.; Lammens, K.; Bartho, J. D.; Grädler, U.; Fuchß, T.; Pehl, U.; Alt, A.; van de Logt, E.; Hopfner, K. P. Molecular Basis of Human ATM Kinase Inhibition. *Nat. Struct. Mol. Biol.* **2021**, *28* (10), 789−798.

(35) Demarta-Gatsi, C.; Donini, C.; Duffy, J.; Sadler, C.; Stewart, J.; Barber, J. A.; Tornesi, B. Malarial < scp > PI4K</Scp> Inhibitor Induced Diaphragmatic Hernias in Rat: Potential Link with Mammalian Kinase Inhibition. *Birth Defects Res.* **2022**, *114* (10), 487−498.

(36) World Health Organization. Global technical strategy for malaria 2016−2030. https://apps.who.int/iris/rest/bitstreams/1357541/retrieve.

(37) Friesner, R. A.; Banks, J. L.; Murphy, R. B.; Halgren, T. A.; Klicic, J. J.; Mainz, D. T.; Repasky, M. P.; Knoll, E. H.; Shelley, M.; Perry, J. K.; Shaw, D. E.; Francis, P.; Shenkin, P. S. Glide: A New Approach for Rapid, Accurate Docking and Scoring. 1. Method and Assessment of Docking Accuracy. *J. Med. Chem.* **2004**, *47* (7), 1739−1749.

(38) Lu, C.; Wu, C.; Ghoreishi, D.; Chen, W.; Wang, L.; Damm, W.; Ross, G. A.; Dahlgren, M. K.; Russell, E.; Von Bargen, C. D.; Abel, R.; Friesner, R. A.; Harder, E. D. OPLS4: Improving Force Field Accuracy on Challenging Regimes of Chemical Space. *J. Chem. Theory Comput.* **2021**, *17* (7), 4291−4300.

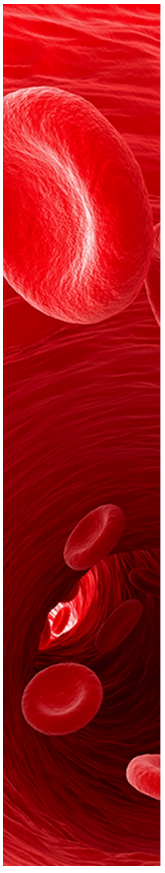

CAS BIOFINDER DISCOVERY PLATFORM™

CAS BIOFINDER HELPS YOU FIND YOUR NEXT BREAKTHROUGH FASTER

Navigate pathways, targets, and diseases with precision

Explore CAS BioFinder

CAS
A division of the American Chemical Society